Ocean Dynamics (2021) 71:757–777
https://doi.org/10.1007/s10236-021-01462-z

Ocean and atmosphere changes in the Caribbean Sea during the twenty-first century using CMIP5 models

David Francisco Bustos Usta[1] · Rafael Ricardo Torres Parra[1]

Received: 29 September 2020 / Accepted: 23 April 2021 / Published online: 14 May 2021

Abstract

Coastal communities around the Caribbean Sea are vulnerable to global warming impacts, partly because of constraints on their adaptive capacity. We use three climate models provided by the Coupled Model Intercomparison Project Phase 5 (CMIP5) under two representative concentration pathways scenario (RCP4.5 and RCP8.5) to assess the trends and spatial behavior of six atmospheric and ocean variables in the Caribbean Basin during the twenty-first century. Atmospheric results are reported from the model ensemble; however oceanic results are reported from ACCESS1.0 model, as its resolution captures mesoscale processes which are important for regional sea level projections. Surface atmospheric pressure and wind do not show significant trends. On the contrary, air and sea surface temperature, surface salinity, and mean sterodynamic sea level have coherent positive trends in the Caribbean Basin, which increase with a greater RCP scenario. Air temperature will probably increase by 2 °C over the preindustrial period during the century. Moreover, sea surface temperature is expected to rise between 1.92° and 3.01 °C in the 1976–2005 to 2071–2100 period. The Caribbean Sea warming will have the potential to extend the hurricane season, increase the frequency of tropical storms, and intensify coral bleaching events. In the same period, mean sterodynamic sea level is expected to rise in the basin between 32.53 and 43.25 cm, depending on the RCP scenario used. The strongest trend expected in 2005-2100 is 50.84 ± 1.48 cm cy^{-1} under RCP8.5 scenario. Furthermore, the trends appear to accelerate since the last century in the basin. Besides, sterodynamic sea level rise would account for slightly over half of the total sea level rise in the Caribbean, after land-ice melting among other contributions not accounted by CMIP5 models are included. These trends have the potential to exacerbate flooding and erosion, putting at risk coastal areas, including low-elevation islands such as some in the San Andres and Providencia Archipelago.

Keywords Climate change · Mean sea level rise · Colombia basin · San Andres and Providencia Archipelago

1 Introduction

For over a century, the earth's climate has been changing as a consequence of greenhouse gas increase in the atmosphere. Climate change impacts include global warming, sea level rise, alterations in atmosphere, and ocean dynamics, among others. Moreover, climate change and its related impacts have large regional differences. Because atmospheric greenhouse gases are expected to increase in the future, climate change impacts are expected to strengthen, increasing threats to the planet and society (IPCC 2014a). Coastal areas are especially vulnerable to climate change, because sea level rise will increase flooding, accelerate erosion, and modify storms in some regions, threatening human welfare and causing great economic losses (IPCC 2014a; Lowe et al. 2004). That is the case in the Caribbean Sea, where sea level extremes in the period 1910–2010 had strong trends caused by mean sea level rise, suggesting that flooding events will become more frequent in the future (Torres and Tsimplis 2014). Therefore, it is necessary to address expected ocean and atmosphere changes across the Caribbean Sea in the twenty-first century

Responsible Editor: Alejandro Orfila

This article is part of the Topical Collection on the *International Conference of Marine Science ICMS2018, the 3rd Latin American Symposium on Water Waves (LatWaves 2018), Medellin, Colombia, 19-23 November 2018 and the XVIII National Seminar on Marine Sciences and Technologies (SENALMAR), Barranquilla, Colombia 22-25 October 2019.*

✉ David Francisco Bustos Usta
dfbustos@uninorte.edu.co

Rafael Ricardo Torres Parra
rrtorres@uninorte.edu.co

[1] Grupo de Investigación en Geociencias GEO4, Departamento de Física y Geociencias, Universidad del Norte, km 5 vía, Puerto Colombia Barranquilla, Colombia

to formulate adequate regional risk mitigation plans for the coastal zone.

Coupled climate models have been created to assess future climate behavior. Global general circulation models (Atmosphere-Ocean General Circulation Models or AOGCMs) simulate dynamic conditions of physical processes of the ocean, atmosphere, cryosphere, and land, including their interactions. These models are considered the best current tool to evaluate the response of earth's climate system to various radiative scenarios related to greenhouse gas concentrations in the atmosphere (IPCC 2014a). Results of AOGCMs run by different research groups have been evaluated in the Coupled Model Intercomparison Project (CMIP). In this paper, results of the CMIP Phase 5 models (Taylor et al. 2018) are reported.

The Caribbean Sea is in a tropical region (Fig. 1), with ~ 90% of the sea surrounded by continental and island landmasses (Gyory et al. 2005). Coastal communities are vulnerable to global warming because of the small islands and developing countries in the basin, with constraints on adapative capacity (Nicholls et al. 2007). The sea is connected to the Gulf of Mexico through the Yucatan Channel on the northwest and the Atlantic Ocean on the north and east. The San Andres and Providencia Archipelago is composed of nine islands within the Colombia Basin (Table 1). The climate is regulated by the meridional position of the Intertropical Convergence Zone (Andrade 2000), creating a windy-dry season (December–April) and rainy-warm season (August–October) (Angeles et al. 2010; Etter et al. 1987), with different regional ocean responses in the basin (Torres and Tsimplis 2012). Trade winds from east to west predominate across the sea (Hastenrath 1968). A dominant low level jet around 15°N in the Venezuela and Colombian basins strengthens in the windy season, reaching speeds of ~ 12 ms^{-1} (Andrade 2000).

Mean sea surface temperature in the Colombian basin has a range between 26 °C in the dry season and 29 °C in the rainy season. Spatial variations show minimum values (~25.5 °C) near La Guajira, with maxima (~29.5 °C) in the Darien and Mosquito gulfs (Ruiz and Beier 2012). Sea surface salinity in the Colombian Basin is lowest in the rainy season and has spatial variations, with saltier water near La Guajira and fresher in the Darien and Mosquito gulfs (Beier et al. 2017). Cold and salty surface waters near La Guajira indicate local upwelling forced by the trade winds, whereas warm and fresher waters in the Darien and Mosquito gulfs coincide with the cyclonic Panama Colombia Gyre forced by wind stress curl (Montoya-Sanchez et al. 2018; Torres and Tsimplis 2012; Mooers and Gao 1996). The Panama-Colombia countercurrent detaches from the eastern side of the gyre, following the Colombian coast toward the northeast (Beier et al. 2017). However, surface currents in the basin are dominated by the Caribbean Current, which flows in the northwest direction (Richardson 2005; Nystuen and Andrade 1993).

Knowledge of atmospheric and ocean behavior in the Caribbean Sea has improved in the last decade, by assessing variables such as atmospheric temperature, pressure and wind (Hamed and Yunfang 2020; Rodriguez-Vera et al. 2019; Montoya-Sanchez et al. 2018), sea surface temperature and salinity (Beier et al. 2017; Ruiz and Beier 2012), and mean sea level rise (Torres and Tsimplis 2013). However, little is known about projected regional changes of these variables in the twenty-first century under various possible Representative Concentration Pathways (RCPs)' scenarios forcing climate change. Such information is necessary to determine expected

Table 1 Location of islands in San Andres and Providencia Archipelago (DIMAR 2019)

Name	Notation[1]	Latitude (N)	Longitude (W)	Maximum height (m)[2]	2071–2100 sea level rise (cm)[3]	
					RCP4.5	RCP8.5
San Andres	S	12.55°	81.72°	100.0	32.44	44.71
Albuquerque	A	12.17°	81.84°	1.5	32.31	44.68
Bolivar	B	12.40°	81.45°	2.0	32.27	44.77
Providencia	P	13.35°	81.38°	360.0	32.25	44.65
Roncador	R	13.57°	80.08°	4.0	32.56	45.49
Serrana	Sra	14.28°	80.37°	9.8	32.41	44.57
Quitasueño	Q	14.38°	81.15°	1.5	32.19	44.02
Serranilla	S-illa	15.80°	79.83°	8.0	31.86	43.71
Bajo Nuevo	B-N	15.83°	78.67°	2.0	31.78	43.52

[1] Notation as indicated in Fig. 1

[2] Referred to mean sea level

[3] Referred to 1976-2005 sea level from ACCESS1.0 model

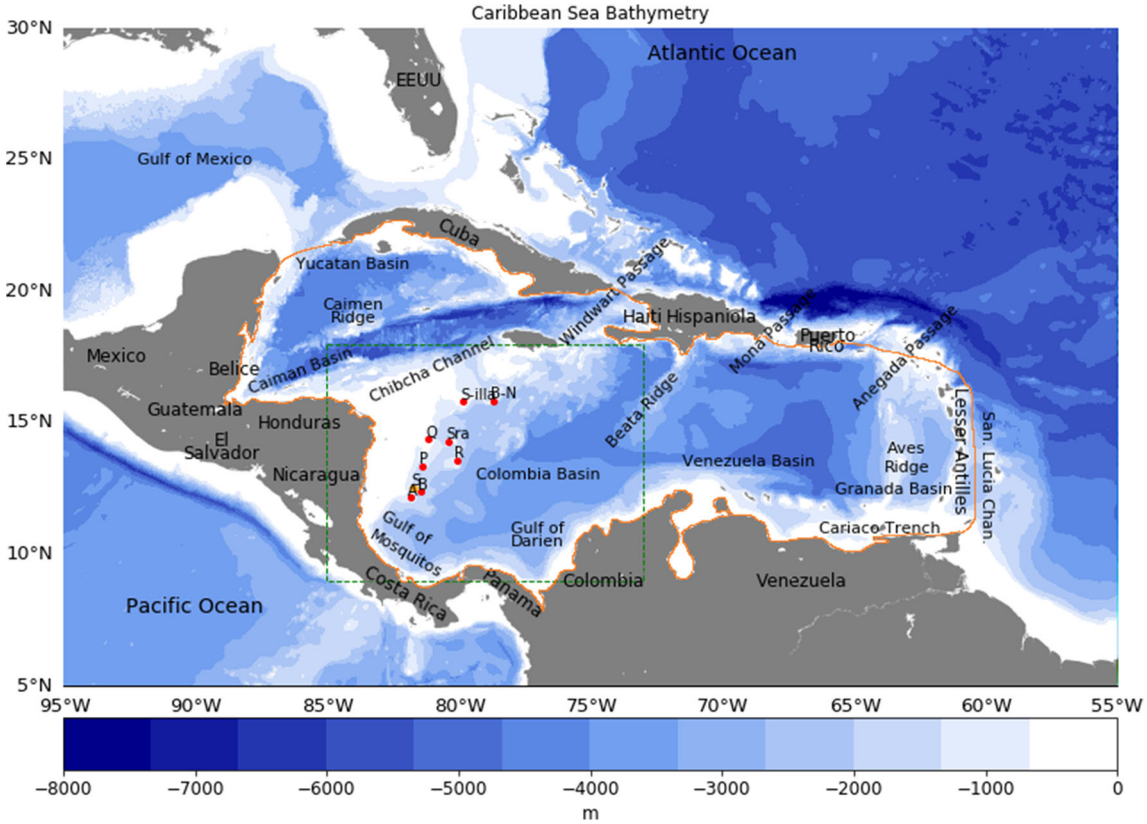

Fig. 1 Map of Caribbean Sea. Bathymetric data from GEBCO (2019). Green rectangle indicates area shown in Fig. 10, including location of San Andrés (yellow star) and other islands (red dots) of the San Andres and Providencia Archipelago. Notation of islands is indicated in Table 1. Red polygon indicates Caribbean Sea limits used to obtain spatial averages of variables.

behavior during the next eight decades of the most important atmosphere and ocean variables and their dependence on various RCP scenarios. This knowledge will allow better understanding of future regional impacts necessary to develop accurate adaptation and mitigation plans, to reduce risk and economic costs of climate change in the Caribbean region.

Therefore, the main objective of this work is to assess the behavior of atmospheric pressure, ambient temperature, wind, ocean temperature, and salinity at the ocean surface, as well as mean sea level in the Caribbean Sea in the twenty-first century. We used results from models ACCESS1.0, CSIRO-Mk3.6, and MIROC5 of CMIP5, under two Representative Concentration Pathway (RCP4.5 and RCP8.5) scenarios. Toward our objective, this paper is organized as follows. Section 2 describes the datasets and methods used. Section 3 presents the results, with a description of the behavior of each of the variables for the two RCP scenarios, including a discussion to contextualize the results. In Section 4, a summary and conclusions are presented.

The main contributions of this work include air and sea surface temperature increase in the Caribbean Sea expected through the present century, regardless of the radiative scenario used. Such temperature trends might lengthen the hurricane season and increase hurricane frequency, as well as increase coral bleaching events, putting at risk these important ecosystems in the Caribbean region. Similarly, mean sea level will continue to rise, intensifying flooding events and coastal erosion. Furthermore, small low islands, such as some in the San Andres and Providencia Archipelago, will be at risk of complete submersion by the end of the century.

2 Data and methods

We analyzed atmospheric pressure (SLP), air temperature (Ta), and winds at sea level, as well as sea surface temperature (SST), sea surface salinity (SSS), and mean sea level for different periods between 1850 and 2100. We used a CMIP5 "historical" run before 2005. RCP4.5 (intermediate) and RCP8.5 (worst) greenhouse gas concentration scenario projections were used between 2005 and 2100. RCP scenarios are named according to radiative forcing target level for 2100. RCP4.5 indicates that radiative emission rate increases from 1.5–2 Wm^{-2} in 2006 to a peak around 2040 and then declines for the rest of the century to 4.5 Wm^{-2} (equivalent to 650 ppm of CO_2) (Vuuren et al. 2011). RCP8.5 has that the radiative

emission rate never stabilizes and increases to ~ 8.5 Wm^{-2} (equivalent to 1370 ppm of CO_2) by 2100, with an increase of ~ 5.5–6 Wm^{-2} with respect to 2006 (Vuuren et al. 2011). Data and model description were accessed from the Program for Climate Model Diagnosis and Intercomparison (PCMDI) (http://cmip-pcmdi.llnl.gov/mips/cmip5/). Model data were downloaded from the Earth System Grid Federation (https://esgf-node.llnl.gov/projects/cmip5/).

Spatial assessment of the variables for the Caribbean was our principal interest, especially sea level as it responds to several atmospheric and oceanic variables reviewed in the study. However, some limitations to assess regional sea level arises because the oceanic components of the latest climate models used for the sea level projections do not explicitly resolve the mesoscale processes in the ocean (Penduff et al. 2010; Serazin et al. 2015). Only some effects of these processes are represented in these models, which generate errors in the circulation processes that affect the regional sea level projections. Therefore, adequate sea level projections in regions such as the Caribbean Sea can only be obtained with high-resolution models that are able to capture mesoscale processes (van Westen et al. 2020). Consequently, the normal approach using a large number of models to reduce uncertainty, might not necessarily provide the most accurate results, as many of them have a coarse ocean resolution on the Caribbean Sea. We decided to have a different approach, selecting three models, which had a good performance against CMIP5 models ensemble as well as a good ocean resolution. To select the models, we examined five criteria as presented in an annex at the supplemental material.

Following these criteria, we selected three models that showed good global and regional performance:

(1) Commonwealth Scientific and Industrial Research Organization (CSIRO) and Bureau of Meteorology, Australia (ACCESS1.0). It has a spatial resolution of 1.875° in longitude and 1.250° in latitude for the atmospheric component (Dix et al. 2012). For the oceanic component, it uses the Arakawa B-grid (Arakawa and Lamb 1977) with zonal and meridional resolution of 1° with three refinements, the most important at the equator with 1/3° (Bi et al. 2012).
(2) Commonwealth Scientific and Industrial Research Organization in collaboration with the Queensland Climate Change Centre of Excellence (CSIROMk3.6). It has a spatial resolution of 1.865° in latitude and 1.875° in longitude for the atmospheric component and 0.9° in latitude and 1.875° in longitude for the oceanic component (Collier et al. 2011).
(3) Atmosphere and Ocean Research Institute (The University of Tokyo), National Institute for Environmental Studies, and Japan Agency for Marine Earth Science and Technology (MIROC5), with a spatial resolution of 1.401° in latitude and 1.406° in longitude for the atmospheric component and 0.5° in latitude and 1.406° in longitude for the oceanic component (Watanabe et al. 2010).

To report the atmospheric projections, we used results from the three-model ensemble, in order to obtain a more robust projection. These atmospheric variables have a similar resolution and coverage from the three models and do not depend strongly on the model resolution. For completeness, the atmospheric projections from ACCESS1.0 are included in the supplementary material (Figure S1). The model ensemble was obtained by interpolating and averaging each model results to a common grid (MIROC5) with the smaller spatial coverage to avoid errors introduced by extrapolation. In the contrary, we report ocean projections from ACCESS1.0. For completeness, ocean results from the models ensemble are included in the supplemental material (Figures S2 and S3). This decision was made as we believe that ocean projections from ACCESS1.0 overcome results from the model ensemble due to the following reasons. (1) As previously mentioned, accurate sea level projections for the Caribbean require high-resolution models to capture mesoscale processes (van Westen et al. 2020). The highest model resolution is used by the oceanic component ACCESS-OM MOM4p1, with a refinement of 1/3° between 10°N and 10°S (Bi et al. 2012). (2) We assessed the three models' spatial results for 1993–2005 using average satellite measurements of sea surface temperature from the COBE mission (Tokyo Climate Center 2020) and sea surface salinity from the Aquarius mission for 2000–2005 (Jet Propulsion Laboratory 2020). Satellite data was linearly interpolated to model nodes. Spatially averaged least differences with the observations were obtained from ACCESS1.0. This model underestimated Caribbean surface temperature by 0.34 °C (the only model with a difference < |1.0|°C) and overestimated surface salinity by 0.17 PSU (the only model with a difference < |0.2| PSU). 3) Ocean mean circulation patterns in the Caribbean were computed using monthly files from OSTM/Jason-2 absolute dynamic topography anomalies for the 1993–2005 period (NOAA 2020a) and compared with mean sea level height above the geoid (SSH). ACCESS1.0 was the model that best reproduced regional circulation patterns and the only one able to reproduce the mesoscale Panama-Colombia Gyre (Bustos 2020). (4) The model ensemble has a smaller ocean spatial coverage losing information near the coasts (e.g., Figure S2).

Two variables are used in the AOGCMs to assess mean sea level. ZOSGA represents the global average of steric sea level (Steric SSH) that is affected by thermal expansion, changes in salinity (Landerer et al. 2014), and water flows between atmosphere, land, cryosphere, and ocean, maintaining earth's water total volume (IPCC 2014c). ZOS, defined as sea level height

above the geoid (SSH), is used to obtain regional changes of dynamic sea level, taking into account the redistribution of mass and changes in circulation (Meyssignac et al. 2017; Yin 2012). To assess total changes in local sea level, these two variables were added (Huang and Qiao 2015) and reported as sterodynamic sea level (SDSL) following van Westen et al. (2020).

Climate models often exhibit spurious trends that are unrelated to external forcing and internal climate variability, especially in oceanic variables. We calculated and removed this model drift from oceanic variables in the Caribbean using the models piControl simulation with a 500-year length for ACCESS1.0 and CSIRO-Mk3.6 as well as 670-year for MIROC5. We applied the full linear drift method recommended by Sen-Gupta et al. (2013). Annual time series were obtained by averaging monthly data from the AOGCMs. To evaluate Caribbean Sea regional behavior, we calculated the spatial mean and standard deviation from all model nodes in the study area (red polygon in Fig. 1). We found time series trends fitting a simple linear regression model, with an intercept using ordinary least squares. Significant error of each estimation was calculated at a 95% confidence level. Serial correlation was not used for the analysis; as consequence, the 95% confidence intervals may be slightly narrower. To compute anomalies, the reference period (1976–2005) was subtracted from the average midcentury (2021–2050) and end of the century (2071–2100) values, with the aim to reduce the interannual variability that could induce bias in the results.

3 Results and discussion

3.1 Surface air temperature (Ta)

3.1.1 Performance in present climate

All models indicated positive and statistically significant trends for Ta across all periods analyzed (Table 2). The weakest trends from all models (0.14 ± 0.07 to 0.34 ± 0.10 °C cy^{-1}) were for the 1850–2005 period (Fig. 2a). For 1960–2005, which represents a more industrialized planet, the trends were between 0.98 ± 0.53 and 1.80 ± 0.74 °C cy^{-1}. The Ta spatial average from the model ensemble in 1976–2005 for the Caribbean was 26.08 ± 0.21 °C with the spatial behavior shown in Fig. 3a.

Ta warming trends in the Caribbean produced by the historical model run are in good agreement with regional trends determined from in situ data for various periods (Peterson et al. 2002; Stephenson et al. 2014; Jones et al. 2016).

3.1.2 Variable projection

The strongest Ta trends were in the projection periods, with values from 1.98 ± 0.44 to 2.87 ± 0.53 °C cy^{-1} (RCP4.5) and 3.15 ± 0.85 to 3.61 ± 0.39 °C cy^{-1} (RCP8.5) for 2005–2050. For 2005–2100, the trends were between 1.60 ± 0.26 and 2.32 ± 0.18 °C cy^{-1} (RCP4.5) and 3.66 ± 0.49 to 4.46 ± 0.39 °C cy^{-1} (RCP8.5). Under RCP4.5, the weaker trends of 2005–2100 relative to 2005–2050 are attributable to radiative emissions decline after 2040 in that scenario. However, because the trends are always positive, Ta is expected to continue to increase in the Caribbean during the entire twenty-first century.

Spatially averaged Ta time series for the Caribbean Sea (Fig. 2a) show large interannual variability under both RCPs scenarios, but they are dominated by the trend after 2005. In addition to the time series, we also assessed Ta spatial behavior for 2021–2050 and 2071–2100 averaged periods from the model ensemble. The Ta spatial average for 2021–2050 (2071–2100) is expected to be 27.14 ± 0.29 °C (28.08 ± 0.14 °C) or 27.33 ± 0.33 (29.40 ± 0.42 °C), under RCP 4.5 or RCP8.5 scenarios, respectively. Differences from the reference period 1976–2005, represent an increase between 1.06 and 2.00 °C (1.25–3.32 °C) under RCP4.5 (RCP8.5) scenario. Ta anomalies for 2021–2050 (respect to the 1976–2005 average) were similar for RCP4.5 (Fig. 3b) and RCP8.5 (Fig. 3d), showing a regional warming of the sea between 1 and 1.5 °C. Ta anomalies for 2071–2100 (respect to the 1976–2005 average) differed between radiative scenarios. Under RCP4.5, temperature will rise between 1.5 and 2.5 °C (Fig. 3c) and ~ 3.5 °C under RCP8.5 (Fig. 3e).

We also studied Ta and SST seasonal changes, because they are important for sea level extremes and sea level sub-regional behavior in the Caribbean (Torres and Tsimplis 2012; Torres and Tsimplis 2014). For coherence, we report results from the ACCESS1.0 model. Under RCP4.5, Ta mean increase is larger from 1976–2005 to 2021–2050 than from 2021–2050 to 2071–2100 (Fig. 4), owing to radiative emission decline after 2040 in that scenario. Although the annual pattern is similar, the annual range decreases from 1.72 °C in 1976–2005 to 1.66 °C in 2071–2100. Under RCP8.5, Ta mean increase is larger from 2021–2050 to 2071–2100 than from 1976–2005 to 2021–2050. Seasonal changes in 2071–2100 are smoothed compared with the variability in 1976–2005 and 2021–2050, and the range decreases, from 1.72 °C in 1976–2005 to 1.63 °C in 2071–2100. Thus, regardless of RCP scenarios used, an increase in Ta is expected in all months for midcentury (2021–2050) and end of the century (2071–2100), maintaining seasonality with maximum values in June (during boreal summer), but reducing the annual Ta range.

The preindustrial Ta mean in the Caribbean Sea (1860–1900) has a spatial mean of 25.72 ± 0.21 °C for the model ensemble (Fig. 2a). In accord with the Paris Agreement (Climate Action Tracker 2020; IPCC 2014a), a 2 °C increase in Ta relative to the preindustrial period has been defined as the limit at which the planet could experience risks and impacts associated with climate change in the attempt to meet the

Table 2 Adjusted trends per century for analyzed atmospheric and oceanic variables, spatially averaged for the Caribbean Sea using two Radiative Concentration Pathways (RCP's) scenarios. Significant trends (95% confidence) are indicated by (*). Models are A (ACCESS1.0), C (CSISOMk3.6), M (MIROC5), and MMM (ensemble). Air temperature (Ta), atmospheric pressure (SLP), and wind speed trends are indicated in °C cy^{-1}, hPa cy^{-1}, and ms^{-1} cy^{-1}, respectively. Sea surface temperature (SST), sea surface salinity (SSS), sea surface above geoid (SSH), global averaged steric sea level (Steric SSH), and local mean sterodynamic sea level (SDSL) trends are indicated in °C cy^{-1}, PSU cy^{-1}, and cm cy^{-1}, respectively

Experiment		Historical		RCP4.5		RCP8.5	
Variable	**Model/Per.**	**1850–2005**	**1960–2005**	**2005–2050**	**2005–2100**	**2005–2050**	**2005–2100**
Atmospheric variables							
Ta	A	0.14 ± 0.07*	1.16 ± 0.46*	1.98 ± 0.44*	1.98 ± 0.15*	3.61 ± 0.39*	3.75 ± 0.13*
	C	0.28 ± 0.17*	0.98 ± 0.53*	2.87 ± 0.53*	2.32 ± 0.18*	3.37 ± 0.48*	4.46 ± 0.39*
	M	0.34 ± 0.10*	1.80 ± 0.74*	2.44 ± 0.87*	1.60 ± 0.26*	3.15 ± 0.85*	3.66 ± 0.49*
	MMM	0.26 ± 0.06*	1.31 ± 0.40*	2.43 ± 0.43*	1.98 ± 0.14*	3.38 ± 0.36*	3.98 ± 0.12*
SLP	A	0.17 ± 0.13*	0.63 ± 0.79	−0.43 ± 0.89	−0.18 ± 0.29	−0.42 ± 0.80	0.46 ± 0.30*
	C	−0.03 ± 0.14	0.30 ± 0.82	−0.37 ± 0.94	−0.37 ± 0.28*	−0.46 ± 0.98	−0.52 ± 0.27*
	M	−0.09 ± 0.14	−0.47 ± 0.98	−0.25 ± 1.14	0.27 ± 0.36	−0.41 ± 1.21	0.44 ± 0.34*
	MMM	0.02 ± 0.08	0.15 ± 0.48	−0.35 ± 0.72	−0.10 ± 0.20	−0.46 ± 0.71	−0.26 ± 0.20*
Wind	A	0.10 ± 0.09*	0.30 ± 0.60	−0.17 ± 0.55	−0.16 ± 0.17	−0.37 ± 0.47	0.12 ± 0.14
	C	−0.05 ± 0.12	0.06 ± 0.53	−0.06 ± 0.70	0.07 ± 0.20	0.07 ± 0.57	0.05 ± 0.16
	M	−0.04 ± 0.08	−0.56±0.45*	−0.04 ± 0.58	0.17 ± 0.19	−0.24 ± 0.71	−0.05 ± 0.20
	MMM	−0.01 ± 0.07	−0.04 ± 0.34	−0.10 ± 0.38	0.04 ± 0.11	−0.19 ± 0.37	0.03 ± 0.10
Oceanic variables							
SST	A	0.08 ± 0.07*	1.01 ± 0.49*	1.82 ± 0.46*	1.85 ± 0.16*	3.40 ± 0.41*	3.36 ± 0.14*
	C	0.25 ± 0.11*	0.95 ± 0.71*	2.62 ± 0.67*	2.14 ± 0.21*	3.10 ± 0.57*	4.17 ± 0.19*
	M	0.03 ± 0.10	0.70 ± 0.63*	3.47 ± 0.53*	2.30 ± 0.22*	4.30 ± 0.46*	5.46 ± 0.21*
	MMM	0.12 ± 0.06*	0.89 ± 0.41*	2.64 ± 0.32*	2.10 ± 0.13*	3.60 ± 0.29*	4.33 ± 0.12*
SSS	A	0.05 ± 0.04*	−0.13 ± 0.24	0.99 ± 0.25*	0.86 ± 0.10*	1.01 ± 0.24*	1.76 ± 0.10*
	C	0.06 ± 0.05*	0.43 ± 0.25*	0.86 ± 0.30*	0.91 ± 0.10*	1.01 ± 0.28*	1.34 ± 0.18*
	M	0.14 ± 0.03*	0.41 ± 0.15*	0.77 ± 0.15*	0.44 ± 0.06*	0.73 ± 0.11*	0.78 ± 0.06*
	MMM	0.08 ± 0.02*	0.23 ± 0.12*	0.88 ± 0.32*	0.74 ± 0.06*	0.92 ± 0.11*	1.25 ± 0.05*
SSH	A	2.04 ± 0.44*	2.62 ± 2.90	2.69 ± 2.98	2.36 ± 0.87*	5.08 ± 3.08*	4.82 ± 0.80*
	C	−0.41 ± 0.42	1.16 ± 2.78	5.63 ± 2.33*	−0.75 ± 0.93	1.88 ± 2.87	0.78 ± 0.81
	M	−3.86±0.58*	−0.57 ± 3.07	16.28±2.63*	17.18 ± 0.88*	17.16±3.12*	22.33 ± 1.25*
	MMM	−0.74±0.26*	1.07 ±1.92	8.19 ±1.53*	6.26 ±0.47*	8.04 ± 1.98*	9.31 ± 0.57*
Steric SSH	A	7.38 ± 0.13*	8.83 ± 0.93*	28.26±0.61*	31.21 ± 0.26*	33.53±0.89*	46.01 ± 1.29*
	C	2.85 ± 0.12*	3.37 ± 0.71*	20.59±0.69*	24.77 ± 0.36*	22.16±0.93*	35.20 ± 1.26*
	M	9.40 ± 0.51*	15.21±1.29*	36.18±0.62*	38.82 ± 0.32*	36.86±0.80*	48.61 ± 1.33*
	MMM	6.54 ± 0.24*	9.14 ± 0.89*	28.34±0.54*	31.60±0.29*	30.85±0.81*	43.27±1.29*
SDSL	A	9.42 ± 0.50*	11.45±3.48*	30.95±3.18*	33.56 ± 0.90*	38.60±2.96*	50.84 ± 1.48*
	C	2.44 ± 0.44*	4.53 ± 2.91*	26.21±2.34*	24.02 ± 0.81*	24.04±2.78*	35.97 ± 1.29*
	M	5.54 ± 0.99*	14.64±4.25*	52.46±2.86*	56.00 ± 1.02*	54.02±3.57*	70.94 ± 2.30*
	MMM	5.80 ± 0.43*	10.21±2.43*	36.54±3.07*	37.86 ± 0.46*	38.89±2.22*	52.58 ± 1.55*

sustainable development goals (United Nations 2020). Under RCP4.5, Ta in the Caribbean would be near the limit established by the Paris Agreement 27.72 °C, probably about 2060, whereas under RCP8.5, this limit would be reached after 2040 (Fig. 2a). Therefore, global efforts should continue to keep radiative emissions below the RCP4.5 level, while Caribbean communities should fortify their preparation to mitigate regional climate change effects.

Taylor et al. (2018) studied air temperature and precipitation from 42 CMIP5 models of the Caribbean for the period 1861–2100 under RCP4.5. They further selected 10 models that showed bimodal precipitation with peaks in June and September, including ACCESS1.0, CSIROMk3.6, and MIROC5. Most models indicated that air temperature would attain an increase of 2 °C between 2033 and 2062 relative to the preindustrial period (1861–1900). This indicates that Ta

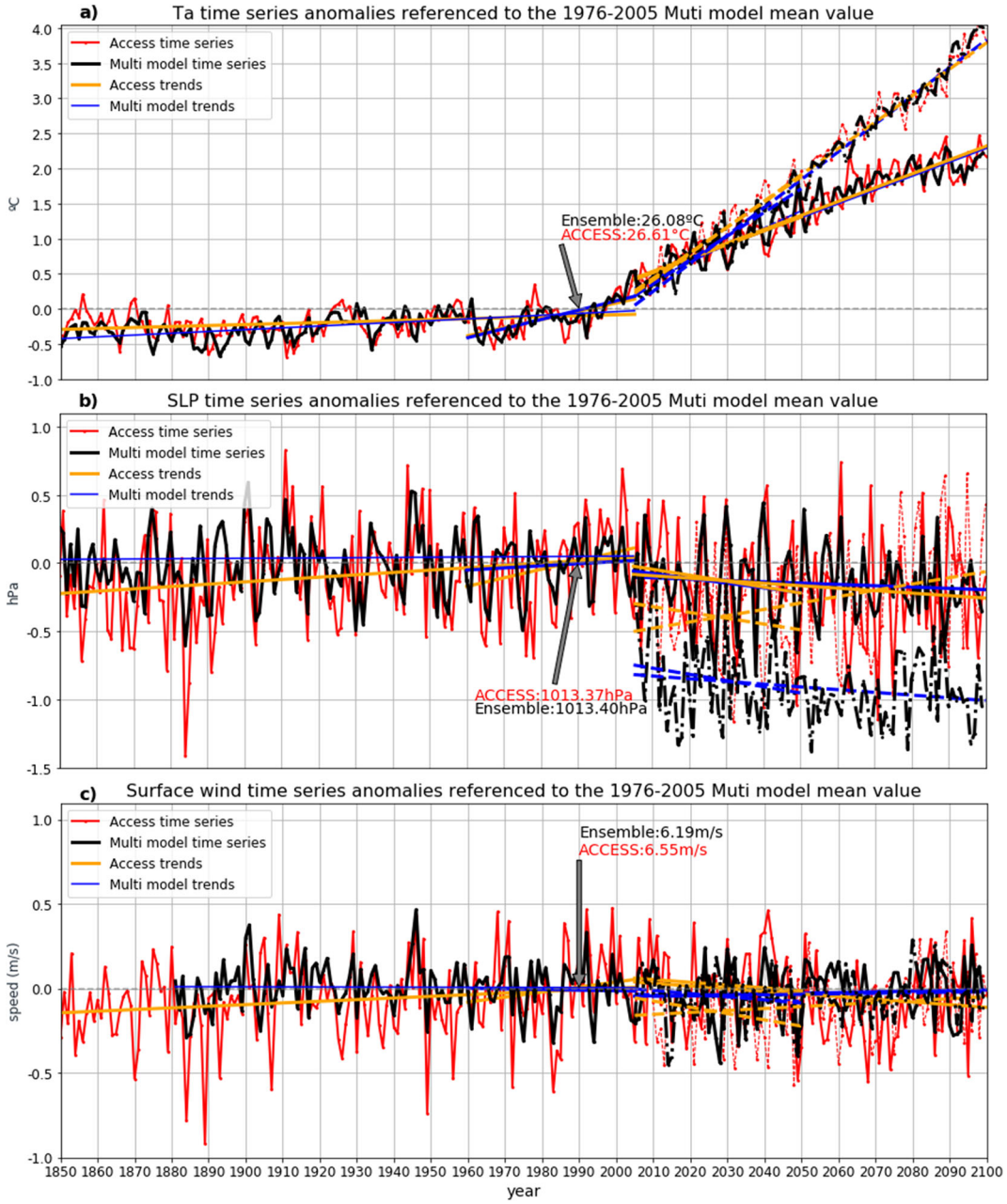

Fig. 2 Time series spatially averaged for the Caribbean Sea from the models ensemble (black) and ACCESS1.0 (red) (**a**) air temperature (°C), (**b**) atmospheric pressure (hPa), and (**c**) wind (ms^{-1}) anomalies referenced to 1976–2005 averaged period (value indicated with the gray arrow). The 1850–2005 results are from historical experiment. The 2005–2100 projection is for RCP4.5 (solid line) and RCP8.5 (dotted line) scenarios. Fitted linear trends are shown for different periods in blue (orange) lines for the models ensemble (ACCESS1.0). Trends value are presented in Table 2

increase according to our model ensemble for the Caribbean is close to the lower limit (smaller Ta trends), as compared with the results from Taylor et al. (2018).

3.2 Atmospheric sea level pressure (SLP)

3.2.1 Performance in present climate

SLP in the Caribbean Sea did not have significant trends for the two historical periods assessed (Table 2), except for ACCESS1.0 with a trend of 0.17 ± 0.13 hPa cy^{-1} in 1850–2005. This indicates that atmospheric pressure in the study area has been steady during the previous century.

For 1976–2005 averaged period, SLP had a value from the models ensemble of 1013.40 ± 0.17 hPa for the Caribbean (Fig. 3f). It gave a southwest–northeast pressure gradient of ~ 10 hPa, between the Darien low pressure (over Panama) and North Atlantic Subtropical Gyre high pressure, resembling typical regional behavior (Andrade 2000).

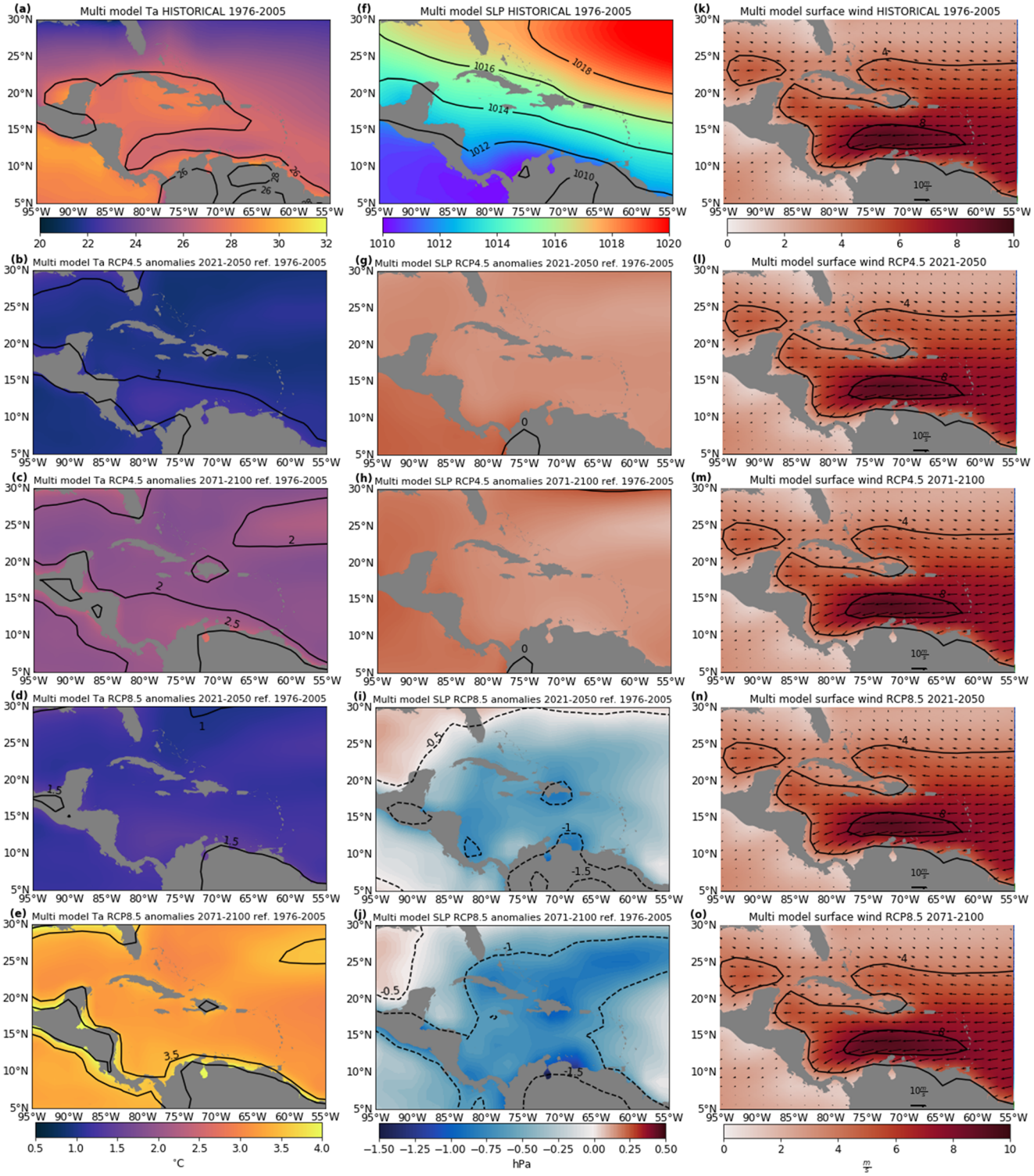

Fig. 3 Air temperature (°C, first column), atmospheric pressure (hPa, second column), and wind (m s^{-1}, third column) spatial behavior in Caribbean Sea from the models ensemble. For 1976–2005 averaged period (first row) after the "historical" run. Temperature and atmospheric pressure anomalies for 2021–2050 relative to 1976-2005 and 2021–2050 mean wind behavior under RCP4.5 are in second row. Third row is as second row but for 2071–2100 anomalies and mean. Fourth and fifth rows are as second and third rows, respectively, but under RCP8.5 scenario

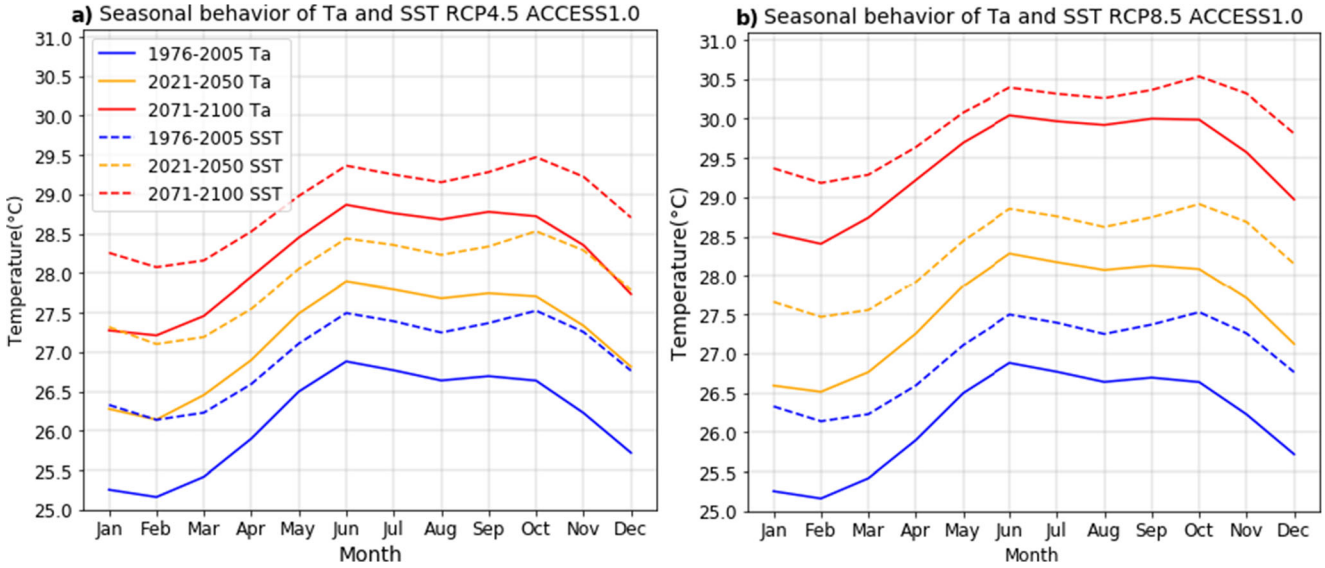

Fig. 4 Seasonal behavior for 1976–2005, 2021–2050, and 2071–2100 averaged periods of surface ambient temperature (Ta) and sea surface temperature (SST) in the Caribbean Sea from ACCESS1.0 model under RCP4.5 (**a**) and RCP8.5 (**b**) scenarios

In the work of Knaff (1997), SLP was analyzed from July to September for certain years between 1950 and 1986, using 11 meteorological stations. Reported SLP values and spatial gradients were similar to those from the models ensemble for 1976–2005 (Fig. 3f).

3.2.2 Variable projection

A similar behavior of trends was observed for the projection periods, regardless of RCP scenario used. Two significant negative trends are present from CSIRO-Mk3.6 for 2005–2100, −0.37 ± 0.28 and, −0.52 ± 0.27 hPa cy^{-1} for RCP4.5 and RCP8.5, respectively (Table 2). There were also significant positive trends from ACCESS1.0 and MIROC5 for 2005–2100 under RCP8.5. However, the model ensemble for the same projection shows negative trends of −0.26 ± 0.20 hPa cy^{-1}, therefore dominated by the CSIRO-Mk3.6 time series. This lack of coherence between models and trends reflects large uncertainty in the model responses for SLP under both scenarios until 2100. Further, spatially averaged SLP time series for the Caribbean Sea (Fig. 2b) were dominated by large interannual variability.

SLP anomalies for 2021–2050 with respect to 1976–2005 were close to zero in the model ensemble, with regional mean of 1013.51 ± 0.29 hPa (Fig. 3 g) and 1012.52 ± 0.27 hPa (Fig. 3i) for the RCP 4.5 and RCP8.5 scenarios, respectively. For 2071–2100, SLP anomalies were also close to zero. For RCP4.5 scenario, the regional mean is 1013.47 ± 0.21 hPa (Fig. 3 h) and under RCP8.5, anomalies could be between 0 and −1.25 hPa between the Yucatan and Venezuela basins, with a regional mean of 1012.67 ± 0.25 hPa (Fig. 3j).

In Section 3.6, we examine sea level trends for the Caribbean Sea. To study the atmospheric pressure contribution to sea level, the inverse barometer effect assumes a 1-cm sea-level increase or decrease for a respective decrease or increase of 1 hPa of atmospheric pressure. This inverse barometer correction has been applied in the Caribbean Sea, because geostrophic control does not impose constraints on water exchanges with the Atlantic Ocean through the straits at time scales longer than 1 day (Torres and Tsimplis 2013). However, as a coherent significant trend was not found in SLP, we assumed that changes in atmospheric pressure will not significantly affect mean sea level trends in the Caribbean during the present century. We could not find studies of SLP in the Caribbean that included a future trend assessment.

3.3 Surface wind

3.3.1 Performance in present climate

Surface wind did not have coherent trends for the historical periods in the Caribbean Sea according to the three models (Table 2). Only two significant trends were found from the historical run. For the period 1850–2005, ACCESS1.0 showed a trend of 0.10 ± 0.09 ms^{-1} cy^{-1}, whereas for 1960–2005, MIROC5 gave a trend of −0.56 ± 0.45 ms^{-1} cy^{-1}. These results indicate that temporal wind variability in the Caribbean is also dominated by large interannual variability (Fig. 2c), as found for SLP. The coherence between wind and SLP behavior corresponds to the dependence of the former on the latter. Therefore, it appears that in the Caribbean atmosphere, the radiative emission rate does not greatly affect SLP or surface wind, whereas it certainly affects Ta.

In the 1976–2005 period, the average wind speed for the Caribbean according to the models ensemble is 6.19 ± 0.15 ms^{-1}, with values > 8 ms^{-1}, indicating the position of the low-

level jet (Fig. 3k) and resembling the typical wind behavior in the basin.

We executed a seasonal analysis of long-term variation of the surface wind, since this variable dominates seasonal changes in the regional ocean circulation (Torres and Tsimplis 2012). Thus, we investigated a wind time series from the dry and windy season (December–January–February) and rainy-warm season (September–October–November) using both RCPs. As expected, wind speed was stronger in the dry season than the rainy season (e.g., 6.53 ± 0.24 ms^{-1} and 5.27 ± 0.18 ms^{-1}, respectively, for 1976–2005 from the model ensemble).

3.3.2 Variable projection

Surface wind did not have coherent trends for projection periods in the Caribbean Sea according to the three models (Table 2), thus reflecting large uncertainty in the model responses until 2100, regardless of RCP scenario used.

Because significant trends in wind speed were not found for the projection periods, the regional wind pattern shows small differences for 2021–2050 and 2071–2100 under both RCP scenarios (Figs 3l–3o), relative to 1976–2005 in the model ensemble. The largest difference was in 2071–2100 under the RCP8.5 scenario, with a regional increase in wind speed and reaching a spatial mean of 6.50 ± 0.19 ms^{-1}.

From the seasonal analysis of long-term variation of the surface wind, we did not find notable changes in wind speed and direction for 2021–2050 and 2071–2100 averaged periods in either season or RCP scenario (not shown). The largest differences (wind speed increase) were in 2071–2100 for the RCP4.5 windy season, with a regional wind speed mean of 7.11 ± 0.24 ms^{-1}.

Costoya et al. (2019) researched projections of wind energy resources in the Caribbean for the twenty-first century. They used seven AOGCM models from CMIP5 (including CSIROMk3.6 and MIROC5), with simulations via regional climate models and downscaling techniques. They found that the maximum annual wind speed increase in the Caribbean would be ~ 0.4 ms^{-1} by 2100 under RCP8.5, referenced to the 2005 value. Thus, their increase in regional wind is greater than that we found with the model ensemble for the same period and RCP (0.25 ms^{-1}).

Evaluating future changes in surface wind is important, because various authors have shown the dominance of wind in the Caribbean Sea circulation (e.g., Montoya-Sanchez et al. 2018; Torres and Tsimplis 2012; Brenes and Saborio 1994; Gordon 1967). We found that regardless of radiative scenario, no significant changes in wind speed or direction are expected in annual or seasonal behavior. Thus, wind-driven changes in the Caribbean ocean circulation during the twenty-first century are not expected to be dominant. Future changes in the Caribbean circulation are assessed in Section 3.6.2.

3.4 Sea surface temperature (SST)

3.4.1 Performance in present climate

Significant and positive trends are found for SST in the historical experiment for the Caribbean Sea in all the models analyzed (Table 2). The only non-significant trend was for 1850–2005, from the MIROC5 model. SST behavior was similar to Ta as expected, owing to heat fluxes between atmosphere and ocean. We found the smallest trends (null to 0.25 ± 0.11 °C cy^{-1}) for 1850–2005, with a noticeable increase over 1960–2005 (0.70 ± 0.63 and 1.01 ± 0.49 °C cy^{-1}). However, in the historical run, significant SST trends do not protrude over interannual variability (Fig. 5a).

SST spatial behavior for 1993–2005 measured by the COBE satellite (Tokyo Climate Center 2020) is homogeneous in the Caribbean Sea, with a spatial mean of 27.29 ± 0.21 °C (Fig. 6d). To the north of the basin, it shows a meridional variation in temperature, decreasing as latitude increases. We compare the satellite measurements with the reference 1976–2005 period from the model. Although they show different averaged periods, we assume that both indicate initial conditions. In the case of the CMIP5 models, as they do not assimilate data, they do not show the historical evolution of the variables. The spatially averaged for the Caribbean from ACCESS1.0 in 1976–2005 underestimates the measured temperature by 0.34 °C, but it is not as homogeneous across the basin; still it shows the meridional temperature decrease north of the Greater Antilles (Fig. 6a). The most notable difference is that in the model, SST increases toward the Darien and Mosquito gulfs. Although the satellite did not measure this temperature increase toward the south of the Colombian Basin in 1993–2005, this area is a strong dilution basin with relatively warm surface temperature compared with water in the central (~ 13°N) Colombian Basin (Beier et al. 2017; Ruiz and Beier 2012).

In the 1976–2005 averaged period, the seasonal SST is 0.79 °C warmer than Ta (Fig. 4), indicating that ACCESS1.0 is able to reproduce atmospheric instability that dominates most of the Caribbean Sea (Linero and Lonin 2015).

Warming trends throughout the Caribbean for the second half of the twentieth century (Table 2) are consistent with those evidenced by Peterson et al. (2002). They reported ocean warming in the Caribbean region for 1950–2000, using time series reconstruction and EOFs. Similarly, Antuña-Marrero et al. (2016), using information reconstructed from the International Comprehensive Ocean–Atmosphere Dataset model, found a trend for 1972–2005 of 1.41 ± 0.67 °C cy^{-1}. Deser et al. (2010) found regional trends in SST with a range of 0.4–1.6 °C cy^{-1} for the period 1900–2008, using observed data and model reconstruction.

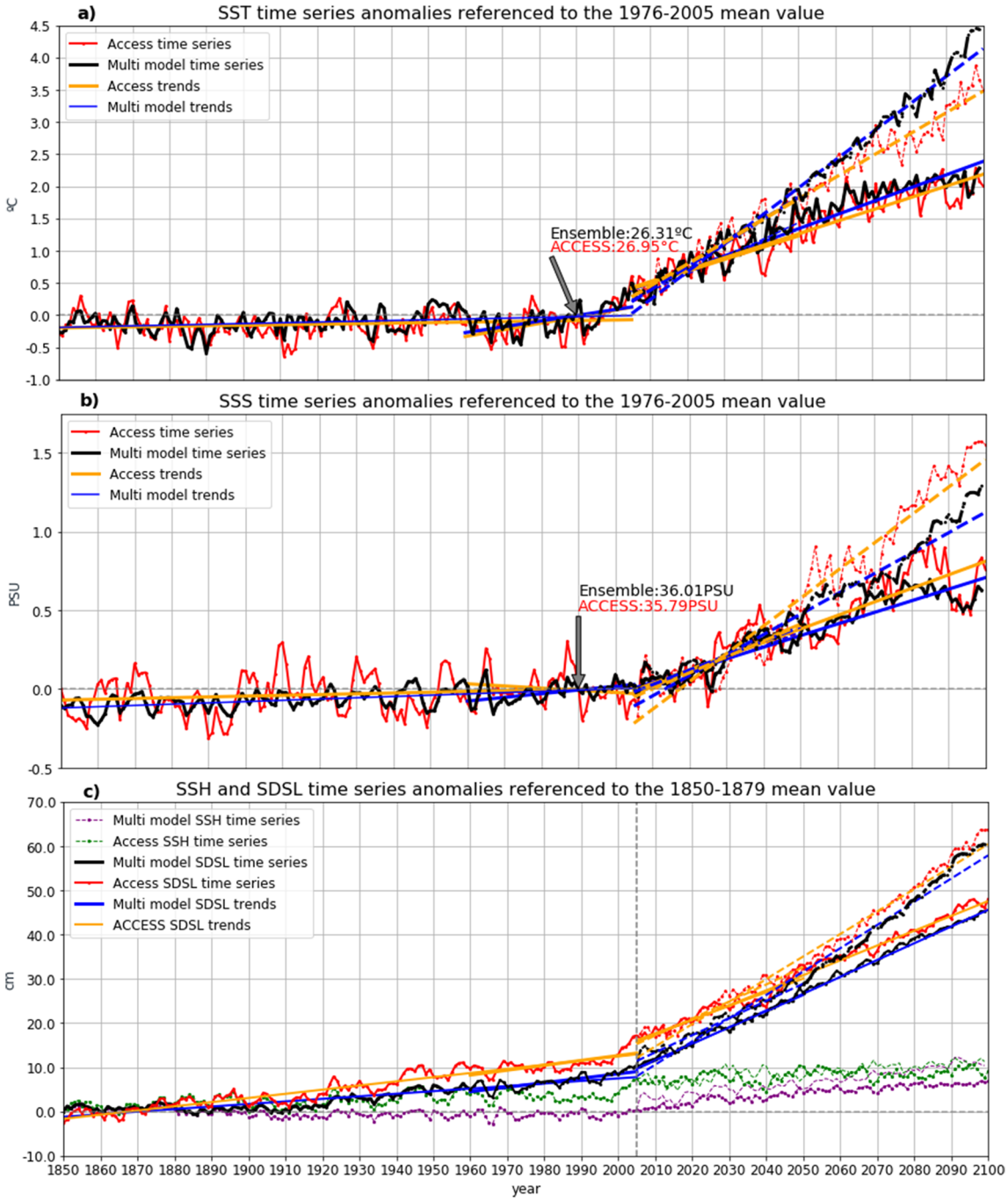

Fig. 5 Time series spatially averaged over the Caribbean Sea from the models ensemble (black and purple) and ACCESS1.0 (red and green): (**a**) sea surface temperature (°C), (**b**) sea surface salinity (PSU), and (**c**) sea surface height and sterodynamic sea level (cm) anomalies referenced to the 1976–2005 and 1850–1879 averaged periods (value indicated with the gray arrow). The 1850–2005 results are from historical experiment. The 2005–2100 projection is for RCP4.5 (solid line) and RCP8.5 (dotted line) scenarios. Fitted linear tends shown for different periods in blue (orange) lines for the model's ensemble (ACCESS1.0). Trends values are presented in Table 2

3.4.2 Variable projection

Significant positive trends dominated SST in all the projected periods analyzed for the Caribbean Sea, regardless of model or RCP scenario used (Table 2). For 2005–2050, trends are between 1.82 ± 0.46 to 3.47 ± 0.53 °C cy^{-1} under RCP4.5. However, trends increased under RCP8.5 to 3.10 ± 0.57 to 4.30 ± 0.46 °C cy^{-1}. For 2005−2100, the trends are between 1.85 ± 0.16 and 2.30 ± 0.22 °C cy^{-1} (RCP4.5) and 3.36 ± 0.14 to 5.46 ± 0.21 °C cy^{-1} (RCP8.5). For the projection periods, SST trends are smaller than Ta trends from the ACCESS1.0 and CSIRO-Mk3.6 models, whereas the opposite occurred

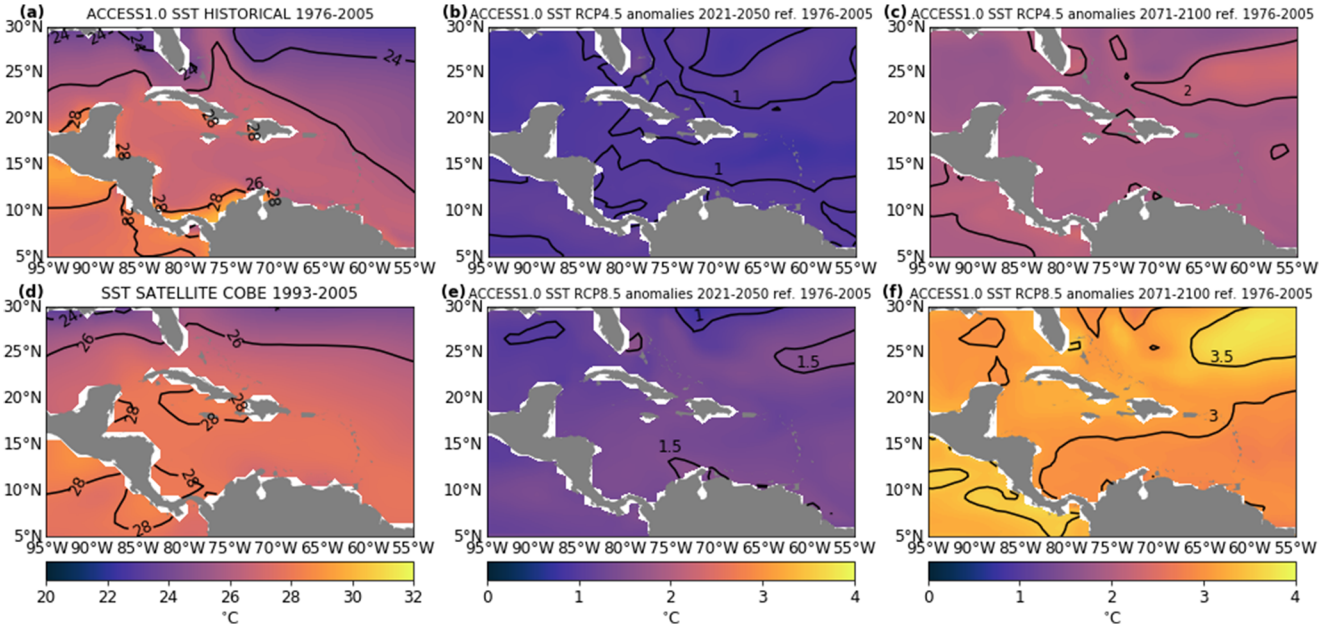

Fig. 6 Spatial behavior of sea surface temperature (SST) (°C) in Caribbean Sea: (**a**) 1976–2005 from model ACCESS1.0 historical run; (**d**) 1993–2005 from satellite (Tokyo Climate Center 2020), with isotherms every 1 °C. Anomalies from 2021 to 2050 and 2071-2100 relative to 1976-2005 averaged period from RCP4.5 in (**b**) and (**c**), respectively, and from RCP 8.5 in (**e**) and (**f**), respectively, showing isotherms every 0.5 °C

with the MIROC5 model. According to the IPCC (2014a), SST is expected to increase globally between 0.70° and 2.40 °C by 2100 under RCP4.5. Therefore, the trends found for the Caribbean are among these values.

Because of this positive trend, by 2071–2100, SST in the Caribbean is expected to be 28.87 ± 0.19 °C or 29.96 ± 0.40 °C in accordance with ACCESS1.0 model under RCP4.5 or RCP8.5, respectively. That represents a temperature increase of 1.92–3.01 °C over the observed value for the 1976–2005 averaged period (Fig. 5a).

SST anomalies in 2021–2050 relative to 1976–2005 under RCP4.5 (Fig. 6b) and RCP8.5 (Fig. 6e) were regionally homogeneous, with an increase between 0.5° and 1.5 °C. For the 2071–2100 period under RCP4.5 (Fig. 6c), anomalies are between 1° and 2.1 °C, and under RCP8.5 between 2.7 and 3.7 °C (Fig. 6f). In both cases, temperature increases are homogeneous in the region, similar to Ta (Figs. 3c–e). SST increase in the Caribbean for 2071-2100 will nearly double that of 2021–2050, which is evidence of the warming trend that will dominate the sea during the twenty-first century.

SST warming trends in the Caribbean produced by the RCP8.5 scenario run are in good agreement with regional trends determined from 26 CMIP5 model ensemble SST trends presented by Alexander et al. 2018), with values between 2.5 and 3.5 °C cy^{-1} for the Gulf of Mexico and the Caribbean for the 1976–2099 period.

The SST annual range is smaller than that of Ta (e.g., 1.39 °C vs. 1.72 °C in 1976-2005). For the period 2021–2050, mean increase in SST under RCP4.5 is 0.98 °C and under RCP8.5 ~ 1.38 °C with reference to the 1976–2005 averaged period (Fig. 4). For 2071–2100, the expected increase from 1976 to 2005 is 1.87 °C under RCP4.5 and 3.01 °C under RCP8.5. The increase from 2021–2050 to 2071–2100 is smaller than 1976–2005 to 2021–2050 for RCP4.5, because this scenario reduces radiative emissions after 2040. SST seasonal behavior for 2021–2050 and 2071–2100 averaged periods indicates a temperature increase in all months as compared with the earlier time series. SST is warmer in June and October and coldest in February in the time series shown in Fig. 4, following the seasonal behavior in the Caribbean Sea (e.g., Torres and Tsimplis 2012).

The studies mentioned in Section 3.4.1 and our results agree on the SST increase in the Caribbean since the beginning of the twentieth century, which is expected to continue through the end of the twenty-first century, regardless of radiative scenario used.

SST increase in the Caribbean Sea during the twenty-first century might affect tropical storms in the basin in two ways, extending the hurricane season and/or increasing storm frequency. However, other factors such as vertical wind shear, atmospheric easterly waves from Africa propagating westward (Goldenberg et al. 2001), or surface wind behavior (Wang and Lee 2007) can influence tropical cyclone activity. The hurricane season in the Caribbean runs from June to November (NOAA: Tropical Cyclone Cimatology, 2020), partially because during these months, SST is warmer (Wang and Lee 2007; Goldenberg et al. 2001). For example, in 1976–2005 averaged period, SST was ≥ 27.36 °C during

hurricane season (Fig. 4). Under both RCP scenarios in 2021–2050 and 2071–2100, all months would exceed this temperature, except February and March under RCP4.5 in 2021–2050 (27.10 and 27.19 °C, respectively). Because warmer sea surface temperatures enhance tropical cyclone formation in the Atlantic (Grinsted et al. 2013), as consequence of SST warming, more months would have sufficient heat in the ocean to permit hurricane formation, which could extend the season in the basin in the future.

In addition, storm frequency could increase in the Caribbean Sea because of the ocean warming in the twenty-first century, regardless of radiative emission scenario. Saunders and Lea (2008) studied the effect of SST increase on the formation of hurricanes in the sea during 1965–2005. They concluded that an increase of 0.5 °C in SST during August and September could cause a ~ 40% increase in the frequency of hurricanes. Under RCP4.5, SST seasonal behavior (Fig. 4) shows an increase in August–September temperature of 0.98° and 1.93 °C for 2021–2050 and 2071–2100, respectively, relative to the 1976–2005 average value. Similarly, under RCP8.5, the SST increase during these months are 1.38 and 3.01 °C for 2021–2050 and 2071–2100, respectively. Therefore, based on the results of Saunders and Lea 2008tropical cyclone frequency could increase by more than 40% by the midcentury period (2021–2050).

Another important consequence associated with the SST increase in the Caribbean Sea is coral bleaching. As ocean temperature rises, corals expel symbiotic algae, affecting their health and turning white (Lough et al. 2018; Eakin et al. 2008; McWilliams et al. 2005). Most coral reefs live in tropical and subtropical waters such as the Caribbean and have substantial biodiversity for the balance of ecosystems (Saravanan et al. 2017). Coral bleaching has increased globally since the early 1980s (Goreau et al. 2000), largely because of the continued increase in global SST (Hughes et al. 2003). The last major global coral-bleaching phenomenon occurred between June 2014 and May 2017, with the loss of hundreds of kilometers of coral reefs (Hartfield et al. 2018).

Changes in SST can trigger coral bleaching events, which has been addressed through different approaches. For example, if SST increases > 1 °C with respect to mean ocean temperature from 1990 to 2017, at least one global strong bleaching episode per decade is anticipated (Ainsworth et al. 2016). Another approach investigated ocean temperatures for 1981–1999, concluding that bleaching events are triggered when SST exceeds a 30.2 °C threshold (Hoegh-Guldberg 1999). In the former case, mean SST in the Caribbean for 1990–2017 (using the historical run and RCP4.5) was 27.20 ± 0.32 °C (Fig. 5a). Thus, SST will exceed 1 °C after ~ 2080 (2059) under RCP4.5 (RCP8.5), facilitating at least one strong coral bleaching event in the basin per decade. In the latter case, the 30.2 °C threshold would be exceeded at the end of the century under RCP8.5 but not RCP4.5 (Fig. 5a). Moreover, the warmer months (> 30.5 °C) between May and November would have the potential to trigger coral bleaching events every year under RCP8.5. Lough et al. (2018) stated that even with limiting global warming to 1.5 °C above pre-industrial levels (Schleussner et al. 2016), it was estimated that after 2050, 70% of the world's reefs will be at risk of severe degradation. According to our study, such a threshold will be exceeded in the region during the present century. Therefore, coral bleaching events due to ocean warming are expected to increase in the Caribbean Sea during the twenty-first century. However, the impact this would have on coral reef health is unclear, because this will also depend on the coral's capacity to adapt to warmer oceans.

3.5 Sea surface salinity (SSS) and density

3.5.1 Performance in present climate

For the historical experiment, positive and significant trends are seen in all periods and models for SSS (Table 2), except for 1960–2005 using the ACCESS1.0 model. The smallest trends were for 1850–2005 (0.05 ± 0.04 to 0.14 ± 0.03 PSU cy^{-1}). However, in the historical run, significant SSS trends do not protrude over interannual variability (Fig. 5b).

SSS in the Caribbean measured from the Aquarius satellite mission between 2000 and 2005 (Jet Propulsion Laboratory 2020) (Fig. 7d) had a spatial mean of 35.62 ± 0.12 PSU. We compare the satellite measurements with our reference 1976–2005 period. The ACCESS1.0 mean for 1976–2005 overestimates by 0.17 PSU the observed salinity field (Fig. 7a). However, the spatial behavior is similar, as the satellite and model show smaller values on the eastern side of the basin, related to the Orinoco freshwater plume (Muller-Karger and Aparicio 1994) and toward the south of the Caribbean, where a dilution basin has been reported owing to strong precipitation and river runoff (Beier et al. 2017). In addition, the Cayman Sea had greater SSS than the eastern Caribbean (Sheng and Tang 2003). The main differences are that the model produced greater SSS in the North Atlantic Subtropical Gyre and near the northern Colombian and Venezuelan coasts, in an area known for its upwelling, thus characterized by greater SSS (Beier et al. 2017).

3.5.2 Variable projection

The largest trends were for the projection periods, with values from 0.77 ± 0.15 to 0.99 ± 0.25 PSU cy^{-1} (RCP4.5) and 0.73 ± 0.11 to 1.01 ± 0.28 PSU cy^{-1} (RCP8.5) for 2005–2050. The largest SSS trends (up to 1.76 ± 0.10 PSU cy^{-1} from the ACCESS model) were for 2005–2100 (Table 2) under RCP8.5 scenario.

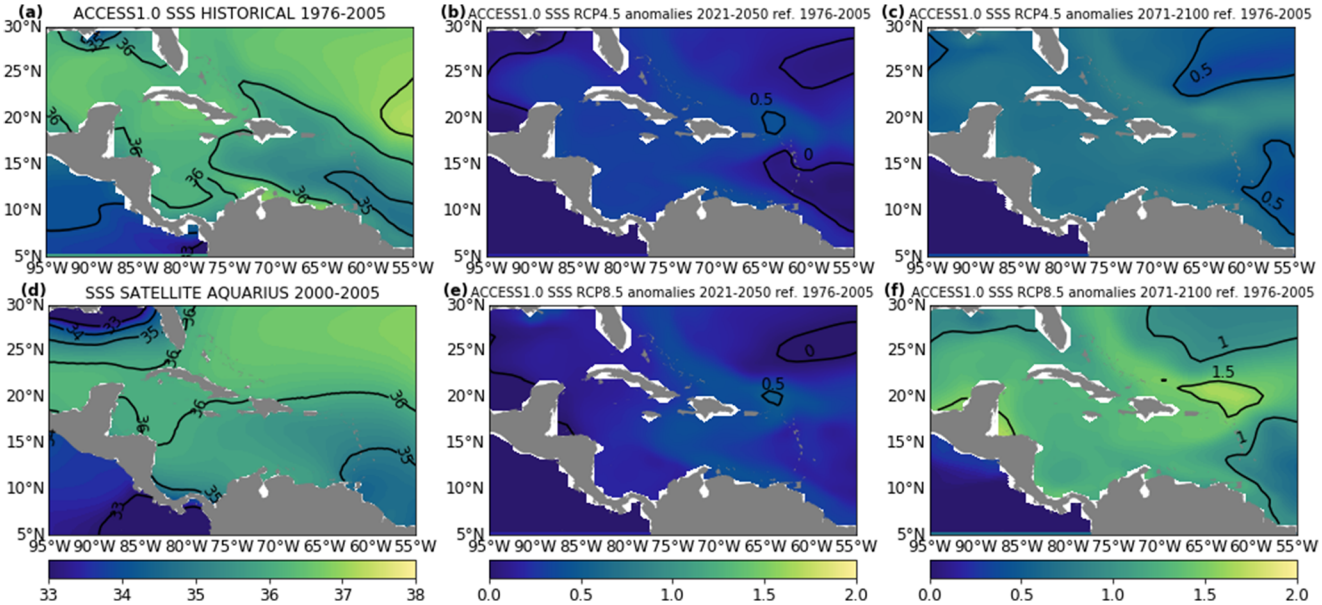

Fig. 7 Spatial behavior of sea surface salinity (SSS) (PSU) in Caribbean Sea: (**a**) 1976–2005 from model ACCESS1.0 historical run; (**d**) 2000–2005 from satellite (Jet, 2020), with isohalines every 1 PSU. Anomalies from 2021 to 2050 and 2071–2100 relative to 1976–2005 averaged period from RCP4.5 in (**b**) and (**c**), respectively, and from RCP8.5 in (**e**) and (**f**), respectively, showing isohalines every 0.5 PSU

According to the ACCESS1.0 model, the expected values of SSS for the 2071–2100 period in the Caribbean are 36.53 ± 0.14 and 37.08 ± 0.16 PSU under RCP4.5 and RCP8.5, respectively (Fig. 5b), both greater than values expected from the model ensemble. The difference of ~ 0.55 PSU between the two RCP scenarios by the end of the twenty-first century indicates the sensitivity of this variable to the radiative forcing scenario used.

For the period 2021–2050 referenced to 1976–2005, SSS increases homogeneously in the Caribbean. Under RCP4.5 (Fig. 7b), SSS increases between 0 and 0.6 PSU, while under RCP8.5 (Fig. 7e), it increases between 0.4 and 0.8 PSU. For 2071–2100 under RCP4.5, SSS increases uniformly in the basin between 0.6–1.1 PSU (Fig. 7c), while under RCP8.5 SSS anomalies are 1–2 PSU, with larger values toward the Yucatan peninsula and Puerto Rico.

Variations in surface density may force changes in circulation. Temperature increase reduces density, whereas salinity increase augments density. Therefore, we analyzed corresponding changes of surface density in the Caribbean as a consequence of consistent SST and SSS positive trends in the twenty-first century. Using ACCESS1.0, under RCP4.5 by 2071–2100, the mean increment of spatially averaged SST (1.92 °C) and SSS (0.74 PSU) relative to 1976–2005 will force a mean increase of 0.11 ± 0.13 kg m^{-3} in surface density. Similarly, under RCP8.5, SST (3.01 °C) and SSS (1.29 PSU) increases will boost surface density by 0.19 ± 0.15 kg m^{-3}. Therefore, according to the model, large changes in the surface density of the Caribbean would not be expected, because SST and SSS trends will partially compensate each other.

The spatial behavior of surface density (not shown) does not change in time. In 1976–2005, 2021–2050, and 2071–2100 averaged periods, regardless of RCP scenario used, minimum surface densities appear to enter the Lesser Antilles moving westward, possibly because of the effect of the Orinoco River. Low surface density is maintained in the southern Colombian basin, associated with warmer temperature and the dilution basin, owing to heavy rainfall and the contribution of rivers such as the Atrato (Chollett et al. 2012; Imbach et al. 2010). Furthermore, greater density indicates the effect of the Guajira upwelling system, apparently persistent under either RCP scenario by 2071–2100. Therefore, regardless of the SST and SSS significant trends shown by the models, surface density spatial patterns currently present in the Caribbean Sea will persist for the remainder of the century, under any radiative scenario.

The Caribbean Sea is a concentration basin where evaporation exceeds precipitation (Yoo and Carton 1990; Etter et al. 1987). The exception is the Colombian basin (Beier et al. 2017). Through satellite observations and numerical models, Grodsky et al. (2014) found that interannual variations of salinity in the Caribbean can reach 0.5 PSU. Significant and positive salinity trends have been reported for the tropical north Atlantic, determined using data from various periods during the twentieth century (Curry et al. 2004; Boyer et al. 2005; Grodsky et al. 2006; Durack and Wijffels 2010). Projections of the increased salinity for 2071–2100 with respect to 1976–2005 under RCP8.5 scenario are slightly greater than the expected increase above 0.8–0.9 PSU in all the subtropical regions of the Atlantic reported by Levang and

Schmitt (2015) and Levang and Schmitt (2020). Their projections were for 2090–2100 under RCP8.5 with respect to the historical 1990–2000 period. Besides, the SSS increase shown in the present study concurs with areas where an increase in SSS is expected as consequence of an excess of evaporation over precipitation (IPCC 2014c).

3.6 Sea level

To study the future behavior of sea level in the Caribbean Sea, we present three analyses for different periods and the two radiative scenarios. First are mean SSH anomalies referenced to the spatial average in the Caribbean, to investigate changes in surface circulation (Fig. 8). Second, we determined spatially averaged trends from SSH, Steric SSH, and sterodynamic sea level (Table 2, Fig. 5c). We also show sterodynamic sea level trends (SDSL) spatial behavior (Fig. 9) to study regional patterns. Third, expected sterodynamic sea level rise for different periods and RCP scenarios is presented, including an impact evaluation for the San Andres and Providencia Archipelago (Fig. 10).

3.6.1 Performance in present climate

The 1993–2005 absolute dynamic topography shows the major mesoscale circulation in the study area (Fig. 8d), including the Caribbean Current, Panama-Colombia Gyre, and Panama-Colombia Countercurrent. We compare the satellite measurements with our reference 1976–2005 period. ACCESS1.0 correctly reproduced the principal circulation patterns (Fig. 8a) using the sea level height anomaly above the geoid (SSH) in this period. The two main differences shown by the model are a stronger sea level gradient in the Colombian Basin and smaller positive values in the northern Cayman Sea, in comparison to the satellite data.

Trends in SSH from the historical run are only significant in ACCESS1.0 (positive) and MIROC5 (negative) in the 1850–2005 period (Table 2). Thus, there was a lack of consistency among the models for SSH trends. In the contrary, Steric SSH trends are significant and positive in all the models and periods from the historical run, dominating all significant and positive SDSL trends, which are larger in 1960–2005 when compared with 1850–2005. SDSL trends are not spatially homogeneous. For 1850–2005, ACCESS1.0 gave larger trends (> 10 cm cy^{-1}) toward the center of the eastern Caribbean (Fig. 9a). Similarly, large trends (> 12 cm cy^{-1}) are seen in the same area for 1960–2005 (Fig. 9d). Although all trends were positive in the Caribbean, they had strong spatial variability, similar to results from other regional sea level studies (e.g., Torres and Tsimplis 2012).

Sen-Gupta et al. (2013) investigated global steric sea level anomalies and trends from 24 CMIP5 models for 1986–2005. ACCESS1.0 model results for the 1960–2005 period were in accordance with the steric SSH rise projections of that work. Using altimetry and tide gauge data, Palanisamy et al. (2012) reconstructed sea level trends in the Caribbean Sea for 1960–2009. They found a spatial mean of ~ 18 ± 5 cm cy^{-1}, larger

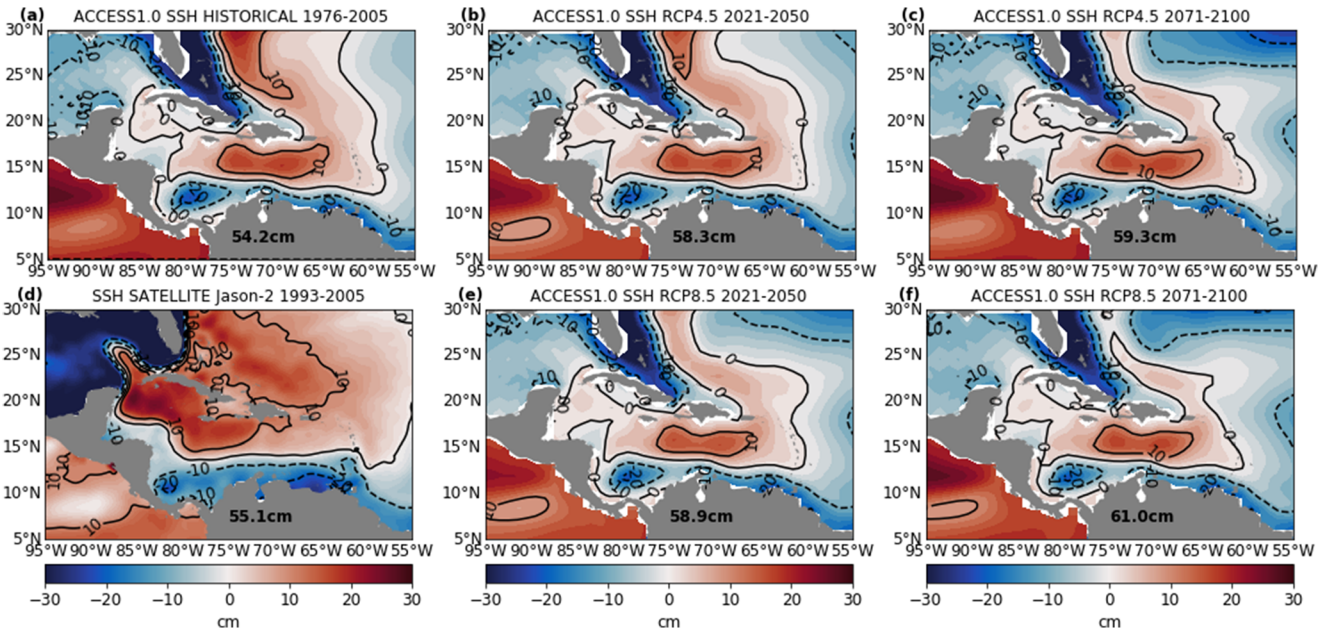

Fig. 8 Spatial behavior of sea level above the geoid (SSH in cm), referred to Caribbean mean value. (**a**) 1976–2005 from model ACCESS1.0 historical run. From RCP4.5 for (**b**) 2021–2050 and (**c**) 2071–2100. From RCP8.5 for (**e**) 2021–2050 and (**f**) 2071–2100. (d) 1993–2005 absolute dynamic topography from OSTM/Jason-2 (NOAA 2020b), referred to Caribbean mean value. Isolines every 5 cm

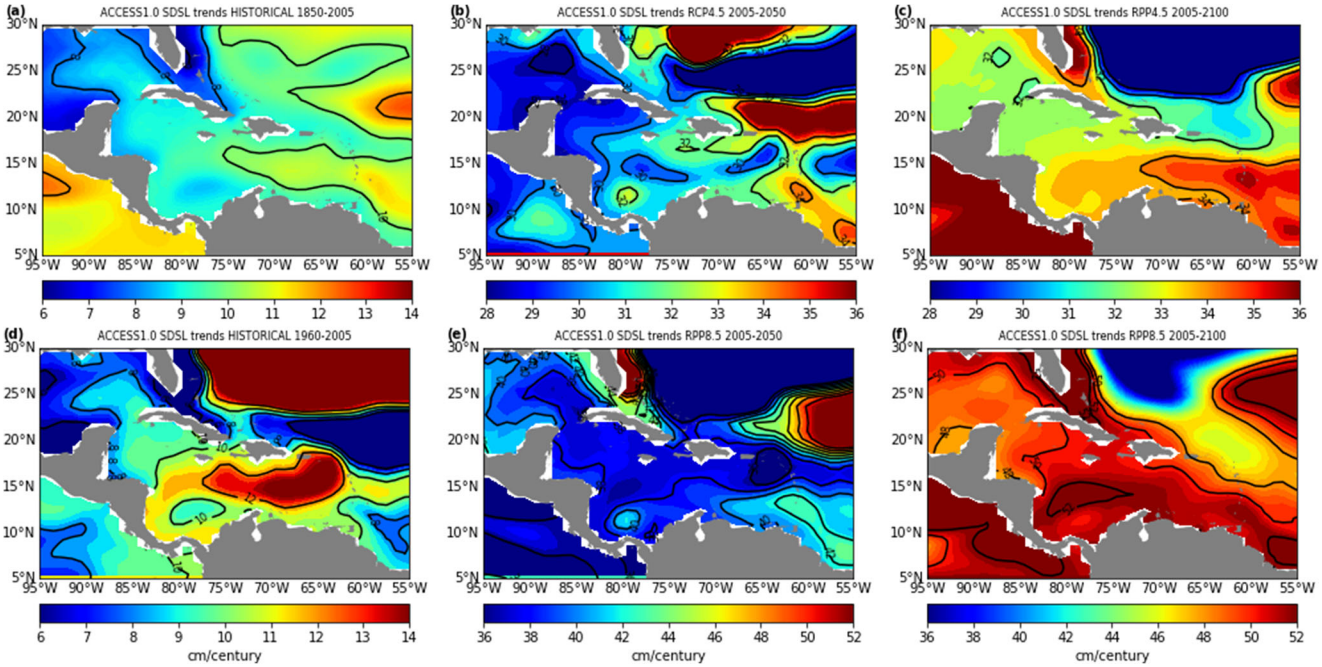

Fig. 9 Sterodynamic sea level trends (SDSL) in cm cy^{-1} for Caribbean Sea from ACCESS1.0 model. Periods (**a**) 1850–2005 and (**d**) 1960–2005 from historical run. Period 2005–2050 using (**b**) RCP4.5 and (**e**) RCP8.5. Period 2005–2100 using (**c**) RCP4.5 and (**f**) RCP8.5. Isolines every 2 cm cy^{-1}. Note different trend ranges in panels

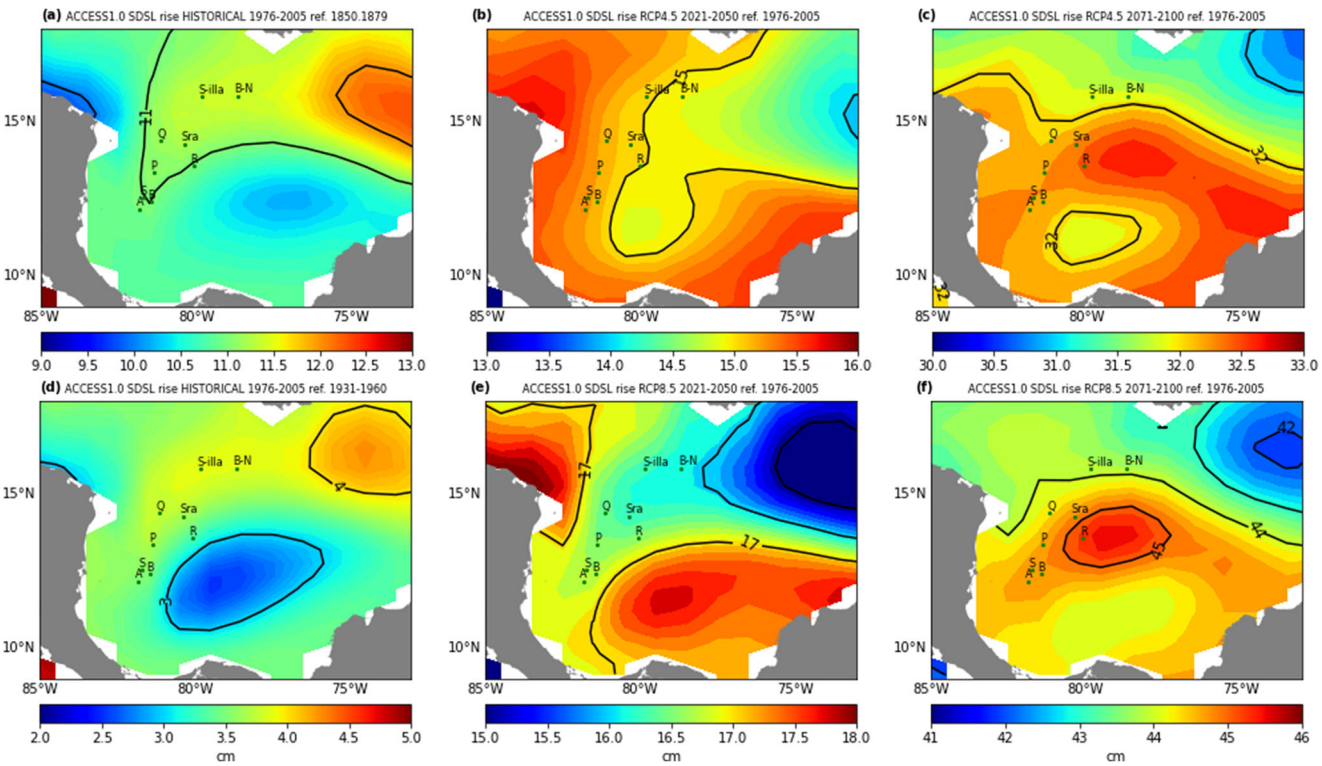

Fig. 10 Sterodynamic sea level rise (SDSL) in (cm) for Archipelago of San Andres and Providencia from model ACCESS1.0. Periods 1976-2005 referenced to (**a**) 1850–1879 and (**d**) 1931–1960 from historical run. Period 2021–2050 using (**b**) RCP4.5 and (**e**) RCP8.5 scenarios. Period 2071–2100 using (**c**) RCP4.5 and (**f**) RCP8.5 scenarios. The last four panels referenced to 1979–2005 averaged period. Isolines every 1 cm. Note different height ranges in each panel

than the SDSL value obtained from ACCESS1.0 for 1960–2005 (11.45 ± 3.48 cm cy^{-1} in Table 2) possibly because the effects of land-ice melting are not included in the model.

3.6.2 Variable projection

Based on a qualitative comparison of the circulation patterns modeled for 2021–2050 and 2071–2100 averaged periods, regardless of radiative scenario, no major changes are expected for the Caribbean (Fig. 8). These results are consistent with small spatial changes in atmospheric pressure and wind for the twenty-first century in the region (Fsig, 3), as well as with small expected changes in sea surface density (Section 3.5). Moreover, spatial averaged SSH trends from ACCESS1.0 are small but significant in some projected periods (Table 2). Therefore, the model indicates minor future basin-averaged rise in the dynamic sea level, with small changes in the circulation patterns.

Larger significant SSH trends were in the projection periods and under RCP8.5 as compared with RCP4.5. Thus, SSH in the Caribbean appears sensitive to the radiative scenario used. Contrary to SSH, all trends in Steric SSH were positive and significant, but similarly, trends were larger in the projection periods under RCP8.5 (Table 2). Consequently, all trends in SDSL were positive and significant for the Caribbean Sea. Larger trends in total sterodynamic sea level were produced by MIROC5 for 2005–2100, with values of 56.00 ± 1.02 (RCP4.5) to 70.94 ± 2.30 cm cy^{-1} (RCP8.5) (Table 2). The fact that the Steric SSH contribution to total sterodynamic sea level trends in the Caribbean was larger than that from SSH indicates that regional sea level rise will be largely due to global temperature increase rather than regional effects (Fig. 5c).

Total sterodynamic sea level trends (SDSL) from ACCESS1.0 in the projected periods were between 30.95 ± 3.18 (RCP4.5, 2005–2050) and 50.84 ± 1.48 cm cy^{-1} (RCP8.5, 2005–2100). The largest trend for RCP4.5 was also for 2005–2100 (33.56 ± 0.90 cm cy^{-1}), but this is smaller than the trend for 2005–2050 under RCP8.5 (38.60 ± 2.96 cm cy^{-1}) (Table 2). Note that SDSL time series for the projection periods are dominated by the trend rather than interannual variability (Fig. 5c). Thus, under any radiative scenario, sterodynamic sea level will continue to rise in the Caribbean during the twenty-first century, but with larger trends under RCP8.5.

Projected SDSL trends in the Caribbean are not spatially homogeneous. For the projection period 2005–2050, trends range between 28 and 33 cm cy^{-1} under RCP4.5 (Fig. 9b) and 35–42 cm cy^{-1} under RCP8.5 (Fig. 9e). In both cases, trends are larger toward the Lesser Antilles and smaller toward the Cayman Sea. Larger trends are around the Panama Colombia Gyre. For 2005–2100, trends are 32–35 cm cy^{-1} under RCP4.5 (Fig. 9c), maintaining the zonal differences. However, the strongest trends are for RCP8.5 scenario, with a range of 48–53 cm cy^{-1} (Fig. 9f), and larger values at the Colombia Basin limit with the Central America Rise.

We also assessed sea level rise for the various periods and two RCP's scenarios using ACCESS1.0 (Figure S4). In 125 years of the historical run (1976-2005 referenced to 1850-1879), the SDSL rose between 10 and 15 cm. The last 45 years of this period (1976-2005 referenced to 1931-1960) the SDSL rose between 3 and 5 cm. In a similar 45-year period of the projection run, (2021-2050 referenced to 1976-2005) the SDSL is expected to rise between 12 and 16 cm (13 and 18 cm) under RCP4.5 (RCP8.5) scenario, thus over twice than the former 45-year period. This behavior indicates an acceleration of SDSL rise in the Caribbean. In nearly 100-year period (2071–2100 referenced to 1976–2005), the SDSL is projected to rise between 32 and 34 cm (42 and 45 cm) under RCP4.5 (RCP8.5) scenario.

According to projections of the IPCC (2014a), global increase in steric sea level by 2081-2100 is expected to be between 15 and 25 cm (25-39 cm) relative to the 1986–2005 period under RCP4.5 (RCP8.5) scenario. Besides, contributions due to dynamic and steric sea level changes in the Caribbean for the same period are estimated between 20 and 30 cm (30–50 cm) under RCP4.5 (RCP8.5) scenario (IPCC 2014b; Church et al. 2007), thus larger than the global steric projection. Using CMIP5 models and probabilistic techniques, regional projections by Jackson and Jevrejeva (2016) for the same period indicated that steric sea level in the Caribbean is expected to rise between 11 and 30 cm (19–45 cm) under RCP4.5 (RCP8.5) scenario. Our results from ACCESS1.0 model for the 2071–2100 relative to the 1976–2005 averaged period (SDSL in Figure S4) are in good agreement with the upper-limit projections obtained in the latter study, and above the upper limit of the global mean steric projections. Bear in mind that the SDSL rise from our study includes a contribution of about 5 cm from the SSH trend (Table 2).

Given the low elevation above mean sea level of some of its nine islands (Table 1), we further examined impacts of SDSL rise in the San Andres and Providencia Archipelago (Fig. 1). In 125 years of the historical run (1976–2005 referenced to 1850–1879), the SDSL rose ~ 11 cm. For 2021–2050 with respect to the 1976–2005 averaged period, the SDSL rise projection is > 14.5 cm (> 16 cm) under RCP4.5 (RCP8.5) scenario in all the Archipelago's islands (Figs. 10 b and e). Note that SDSL rise patterns from the two RCP scenarios are different. In Fig. 10, SDSL trends in the southern Colombia basin seem to be associated to the dynamics of the Panama-Colombia Gyre and thus probably affected by changes in its circulation. Recall that sea level can vary among the islands of the archipelago, owing to its location at the dynamic boundary of the Panama-Colombia Gyre (e.g., Torres et al. 2017).

For 2071–2100 with respect to the 1976–2005 averaged period, the SDSL is projected to rise as much as 32.56 cm under RCP4.5 (Fig. 10c, Table 1) and 45.49 cm (Fig. 10f) under RCP8.5 (Fig. 10f) at Roncador. Although values for the other islands of the archipelago are smaller, they do not differ much. Therefore, at the end of the twenty-first century, islands of lower elevation in the archipelago will be at risk of being submerged most of the time as a consequence of sea level rise and extreme events. In the archipelago, extreme ocean events can be forced by hurricanes (Ortiz et al. 2015), which because of ocean warming can become more frequent (Section 3.4). For example, in the case of inhabited Albuquerque and Quitasueño, where the island maximum height is 1.5 m (Table 1), a sea level rise of ~ 45 cm (RCP8.5) by 2100 will leave only small areas of the islands above mean sea level. Extreme sea level events in the Caribbean are attributable to a combination of tides, atmospheric forcing, mesoscale gyres and the seasonal signal, in addition to a positive trend from sea level rise (Torres and Tsimplis 2014). Thus, by 2100, the combination of sea level rise and extreme sea level events will intensify erosion to a point where entire islands can be submerged below mean sea level. Such events can even have consequences for state sovereignty, because the Law of the Sea does not consider islands that might stop complying with the "island definition" (article 121 in UNCLOS 1994) because of sea level rise.

AOGCM models in CMIP5 do not include the land-ice melting and other smaller contributions to sea level (IPCC 2014c), as their dynamics are difficult to simulate (Henderson-Sellers and McGuffie 2012; Kaser et al. 2006; Dyurgerov and Meier, 2004, b) and beyond the scope of these models. According to IPCC projections for the Caribbean region, the expected changes in total sea level for the 2081–2100 period with respect to 1986–2005 can be estimated between 50 and 60 cm (70–80 cm) under RCP4.5 (RCP8.5) scenario, what fits in the global projections (IPCC, 2014b; Church et al., 2007). Total sea level would include contributions from the steric component but also from land-ice melting, atmospheric loadings, global isostatic adjustment (GIA), and terrestrial water sources. Therefore, SDSL rise reported in this section (Figure S4) contributes for a bit more than half of the total sea level rise expected in the Caribbean Sea by the end of the century. Consequently, sea level rise in the Caribbean, including all components, will be a major threat to the Caribbean Sea low-elevation coastal areas such as some islands in the San Andres and Providencia Archipelago.

4 Summary and conclusions

Three CMIP5 models were used to investigate atmospheric and oceanographic trends (Table 2) during the twenty-first century in the Caribbean Sea, under radiative emission scenarios RCP4.5 and RCP8.5. We used the three-model ensemble to assess the atmospheric variables. However, to report the ocean variables, we used results from ACCESS1.0, due to its better ocean model resolution and coverage, allowing it to capture mesoscale processes what gives it the best performance in the region.

Surface air temperature (Ta) spatial means show significant and consistent positive trends across the three models. A Ta increase of 2 °C referenced to the preindustrial period (25.70 °C), established as a global goal by the Paris Agreement (Climate Action Tracker, 2020), would be reached in the Caribbean by 2060 under RCP4.5, or by 2040 under RCP8.5. Thus, the region will probably exceed this limit during the present century. On the contrary, atmospheric pressure (SLP) and surface wind did not show a uniformity of trends under either of the two RCPs scenarios. Furthermore, we did not find evidence of significant changes in wind during the dry or rainy seasons across the sea.

Spatially averaged trends of SST, SSS, or SDSL for the Caribbean Sea are consistently positive for the present century, regardless of RCP scenario used. Such positive trends are in good agreement with other regional assessments (Alexander et al., 2018, Levang & Schmitt 2020, Jackson & Jevrejeva 2016). However, based on ACCESS1.0 results, the trends are not homogeneous across the basin (Figs. 6, 7, and 9).

The SST spatial average for the Caribbean is expected to increase between 1.92° and 3.01 °C by the end of the twenty-first century with respect to the 1976–2005 averaged period according to ACCESS1.0, depending on the RCP scenario used. However, there is no evidence of large seasonal changes. Such temperature rise could influence tropical storms, such as extending the hurricane season in the basin and/or increasing hurricane frequency by > 40% by the end of the century. Moreover, SST warming can affect coral ecosystems in the Caribbean by increasing and strengthening bleaching events, what might have a strong impact on regional ecosystems and food supplies for coastal communities.

We assessed qualitative anomalies in sea level height above the geoid (SSH), which were steady over the twenty-first century, regardless of RCP scenario used (Figure 8). Therefore, spatial changes in current Caribbean major circulation features are not expected. This is consistent with small long-term changes in atmospheric pressure gradients (spatially uniform inverse barometer effect), surface wind (momentum transfer), and surface density (buoyant fluxes), the latter a consequence of positive trends in SST and SSS, with opposing effects on density.

In the Caribbean Basin, depending on the RCP scenario used, mean sterodynamic sea level is expected to rise between ~ 32.53 and 43.25 cm for 2071–2100 with respect to the reference period of 1976–2005 (Fig. 5c), given trends up to 50.84 ± 1.48 cm cy^{-1}. Trend increases in two consecutive 45-year periods indicate that sea level rise in the Caribbean is

accelerating, consistent with trend evaluation using a 102-year tide gauge time series from Cristobal-Panama, collected mostly during the last century (Torres & Tsimplis, 2013). In addition, when all sea level contributions are accounted (including land-ice melting), Caribbean Sea level rise for the 2081–2100 period with respect to 1986–2005 can be estimated between 50 and 80 cm depending on the RCP scenario (IPCC, 2014a). Such sea level rise by the end of the century will impose a great threat to low-elevation islands, such as some in the San Andres and Providencia Archipelago, and will be at risk of disappearing.

Because of the results of the present study, in particular significant positive trends in air and sea surface temperature and mean sea level, the Caribbean region will likely experience large climate change impacts by the end of the twenty-first century. Therefore, it is important that local communities continue monitoring environmental variables, maintain low radiative emissions, and improve their development of regional mitigation plans.

Supplementary Information The online version contains supplementary material available at https://doi.org/10.1007/s10236-021-01462-z.

Acknowledgments The authors thank two anonymous reviewers for their valuable comments on this paper.

References

Ainsworth T, Heron S, Ortiz J, Peter M, Alana G, Daisie O, Eakin C, William L (2016) Climate change disables coral bleaching protection on the Great Barrier Reef. Science. 352:338–342

Alexander M, Scott J, Friedland K, Mills K, Nye J, Pershing A, Thomas A (2018) Projected sea surface temperatures over the 21st century: Changes in the mean variability and extremes for large marine ecosystem regions of Northern Oceans. Elementa: Science of the Anthropocene 17:6–23

Andrade C (2000). The circulation and variability of the Colombian Basin in the Caribbean Sea. Ph.D. dissertation.

Angeles M, González J, Ramírez-Beltrán N, Tepley C, Comarazamy D (2010) Origins of the Caribbean Rainfall Bimodal Behavior. J Geophys Res 115:D11106. https://doi.org/10.1029/2009JD012990

Antuña-Marrero J, Ottera O, Robock A, Mesquita M (2016) Modelled and observed sea surface temperature trends for the Caribbean and Antilles. Int J Climatol 36:1873–1886

Arakawa A, Lamb V (1977) Computational Design of the Basic Dynamical Processes of the UCLA General Circulation Model. Elsevier pag:173–265

Beier E, Bernal G, Ruiz-Ochoa M, Barton E (2017) Freshwater exchanges and surface salinity in the Colombian basin. Caribbean Sea PloS one 12:1–8

Bi D, Marsland S, Uotila P, O'Farrell S, Fiedler R, Sullivan A, Griffies S, Hirst A (2012) ACCESS-OM: the ocean and sea-ice core of the ACCESS coupled model. Australian Meteorological and Oceanographic Journal 63:213–232

Boyer T, Levitus S, Antonov J, Locarnini R, Garcia H (2005) Linear trends in salinity for the World Ocean, 1955–1998. Geophys Res Lett 32:35–42

Brenes A, Saborio V (1994) Changes in the general circulation and its influence on precipitation trends in Central America: Costa Rica. Ambio. 23:87–90

Bustos D (2020). Atmospheric and oceanic behavior by 2100 in the Caribbean Sea based on CMIP5 climate model projections. Barranquilla: Master Thesis.

Chollett I, Mumby P, Muller-Karger F, Hu C (2012) Physical environments of the Caribbean Sea. Limnol Oceanogr 57:1233–1244

Church J, Woodworth P, Thorkild A, Stanley W (2007) Understanding Sea Level Rise and Variability. EOS Transactions 88:43–47

Climate Action Tracker. (2020). Paris temperature goal. Obtained from the Paris temperature goal. Available at: https://climateactiontracker.org/methodology/paris-temperature-goal/.

Collier Mark, Jeffrey Stephen, Rotstayn Leon, Wong K-H, Dravitzki S., Moeseneder Christian, Hamalainen C., Syktus Jozef, Suppiah R., Antony Joseph, El Zein Ahmed, Atif Muhammad. (2011). The CSIRO-Mk3.6.0 Atmosphere-Ocean GCM: participation in CMIP5 and data publication. 19th International Congress on Modelling and Simulation, Perth, Australia, 12-16 December. Available at: http://mssanz.org.au/modsim2011

CONVEMAR. 1994. Convención de las Naciones Unidas sobre el Derecho del Mar.

Costoya X, Decastro M, Santos S, Sousa M, Gomez-Gesteira M (2019) Projections of wind energy resources in the Caribbean for the 21st century. Energy. 178:356–367

Curry R, Dickson B, Yashayaev I (2004) A change in the freshwater balance of the Atlantic Ocean over the past four decades. Nature. 426:826–829

Deser C, Phillips A, Alexander M (2010) Twentieth century tropical sea surface temperature trends revisited. Geophys Res Lett 37:L10701

DIMAR. (2019). Derrotero de las Costas y areas insulares del Caribe y Pacifico Colombiano. Derrotero de las Costas y areas insulares del Caribe y Pacifico Colombiano.

Dix M, Bi D, Rashid H, Marsland S, O'Farrell S, Uotila P, Kowalczyk E, Sullivan A, Yan Y, Franklin C, Sun Z, Collier M, Rotstayn L, Uhe K, Puri K (2012) The ACCESS coupled model: Documentation of core CMIP5 simulations and initial results. Australian Meteorological and Oceanographic Journal 63:83–99

Durack P, Wijffels S (2010) Fifty-Year Trends in Global Ocean Salinities and Their Relationship to BroadScale Warming. J Clim 23:4342–4362

Dyurgerov M, Meier M (2004). Glaciers and the Changing Earth System: A 2004 Snapshot. 58**:** 1-117.

Eakin C, Lough J, Heron S (2008). Climate Variability and Change: Monitoring Data and Evidence for Increased Coral Bleaching Stress. https://doi.org/10.1007/978-3-540-69775-6_4

Etter P, Lamb P, Portis D (1987) Heat and freshwater budgets of the caribbean sea with revised estimates for the Central American Seas. J Phys Oceanogr 17:1232–1248

GEBCO. (2019). Gridded Bathymetry Data. Gridded Bathymetry Data. Available at: gebco bathymetry resolution

Goldenberg S, Landsea C, Mestas-Nunez A, Gray W (2001) the recent increase in atlantic hurricane activity: causes and implication. Science. 293:474–479

Gordon A (1967) Circulation of the Caribbean Sea. J Geophys Res-Atmos 72:6207–6223

Goreau T, Mcclanahan T, Hayes R, Strong A (2000) Conservation of Coral Reefs after the 1998 Global Bleaching Event. Conserv Biol 14:5–15

Grinsted A, Moore J, Jevrejeva S (2013) Projected Atlantic hurricane surge threat from rising temperatures. Proc Natl Acad Sci U S A 110:5369–5373

Grodsky S, Carton J, Bingham F (2006) Low frequency variation of sea surface salinity in the tropical Atlantic. Geophys Res Lett **33**:16–20

Grodsky S, Johnson B, Carton J, Bryan F (2014) Interannual Caribbean salinity in satellite data and model simulations. J Geophys Res Oceans 120:1375–1387

Gyory J, Mariano A, Ryan E (2005). The Caribbean Current. Oean Surface Current. Available at: https://oceancurrents.rsmas.miami.edu/caribbean/caribbean.html

Hamed D, Yunfang S (2020) Mechanism study of the 2010-2016 rapid rise of the Caribbean Sea Level. Glob Planet Chang 171:10–32

Hartfield G, Blunden J, Arndt D (2018). State of the Climate in 2017. Bulletin of the American Meteorological Society. 99: Si-S310.

Hastenrath S (1968) A contribution to the wind conditions over the Caribbean Sea and Gulf of Mexico. Tellus 21:162–178

Henderson-Sellers A, McGuffie K (2012). The Future of the World's Climate (Second Edition) (Second Edition ed., págs. 1-2). Boston: Elsevier.

Hoegh-Guldberg O (1999) Climate change, coral bleaching and the future of the world's coral reefs. Mar Freshw Res 50:839–866

Huang C, Qiao F (2015) Sea level rise projection in the South China Sea from CMIP5 models. Acta Oceanol Sin 34:31–41

Hughes T, Baird A, Bellwood D, Card M, Connolly S, Folke C, Grosberg R, Hoegh-Guldberg O, Jackson J, Kleypas J, Lough J, Marshall P, Nyström M, Palumbi S, Pandolfi J, Rosen B, Roughgarden J (2003). Climate Change, Human Impacts, and the Resilience of Coral Reefs. Science (New York, N.Y.), 301: 929-33.

Imbach P, Molina L, Locatelli B, Roupsard O, Ciais P, Corrales L, Mahe G (2010) Climatology-based regional modelling of potential vegetation and average annual long-term runoff for Mesoamerica. Hydrol Earth Syst Sci 14:1–17

IPCC. (2014a). Climate Change 2013: The Physical Science Basis. Chapter 9. Evaluation of Climate Models.

IPCC. (2014b). Climate Change 2014: Synthesis Report. A report of the Intergovernmental Panel on Climate Change.

IPCC. (2014c). Climate Change 2013: The Physical Science Basis. Chapter 13. Sea Level Change.

Jackson L, Jevrejeva S (2016) A probabilistic approach to 21st century regional sea-level projections using RCP and High-end scenarios. Glob Planet Chang 146:179–189

Jet Propulsion Laboratory. (2020). Global sea surface salinity data sets. Obtenido de Global Sea Surface Salinity Data Sets. Availale at: https://podaac.jpl.nasa.gov/datasetlist

Jones P, Harpham C, Harris I, Goodess CM, Burton A, Centella-Artola A, Taylor MA, Bezanilla-Morlot A, Campbell J, Stephenson T, Joslyn O, Nicholls K, Baur T (2016) Long-term trends in precipitation and temperature across the Caribbean. Int J Climatol 36:3314–3333

Kaser G, Cogley J, Dyurgerov M, Meier M, Ohmura A (2006) Mass balance of glaciers and ice caps: Consensus estimates for 1961-2004. Geophys Res Lett 33:1–33

Knaff J (1997) Implications of summertime sea level pressure anomalies in the tropical Atlantic region. J Clim 10:789–804

Landerer F, Glecker P, Lee T (2014) Evaluation of CMIP5 dynamic sea surface height multi-model simulations against satellite observations. Clim Dyn 43:1271–1283

Levang S, Schmitt R (2015) Centennial Changes of the Global Water Cycle in CMIP5 Models. J Clim 28:6489–6502

Levang S, Schmitt R (2020) Intergyre Salt Transport in the Climate Warming Response. J Phys Oceanogr 50:255–268

Linero J, Lonin S (2015). Termodinamica para oceanografos. Cartagena: Escuela Naval de Cadetes Almirante Padilla.

Lough J, Andreson K, Hughes T (2018) Increasing thermal stress for tropical coral reefs:1871-2017. Sci Rep 8:6079

Lowe R, Nicholls J, Jason A (2004) Benefits of mitigation of climate change for coastal areas. Glob Environ Chang 3:229–244

McWilliams J, Cote I, Gill J, Sutherland W, Watkinson A (2005) Accelerating impacts of temperature-induced coral bleaching in the Caribbean. Ecology. 86:2055–2060

Meyssignac B, Slangen A, Melet A, Church J, Fettweis X, Marzeion B, Agosta C, Ligtenberg S, Spada G, Richter K, Palmer M, Roberts C, Champollion N (2017) Evaluating Model Simulations of Twentieth-Century Sea-Level Rise. Part II: Regional Sea-Level Changes Journal of Climate 30:8565–8593

Montoya-Sanchez R, Devis-Morales A, Bernal G, Poveda G (2018) Seasonal and intraseasonal variability of active and quiescent upwelling events in the Guajira system, southern Caribbean Sea. Cont Shelf Res 171:97–112

Mooers C, Gao L (1996) Numerical simulation of the Intra Americas Sea, Part I. Trans Am Geophys Union 76:1–19

Muller-Karger F, Aparicio R (1994) Mesoscale processes affecting phytoplancton abundance in the Southeastern Carribean Sea. Cont Shelf Res 14:199–221

Nicholls RJ, Wong PP, Burkett VR, Codignotto JO, Hay JE, McLean RF, Ragoonaden S, Woodroffe CD (2007) Coastal systems and low-lying areas. In: Parry ML et al (eds) Climate Change, 2007: Impacts, Adaptation and Vulnerability. Contribution of Working Group II to the Fourth Assessment Report of the Intergovernmental Panel on Climate Change. Cambridge Univ. Press, Cambridge, U. K., pp 315–356

NOAA. (2020a). Tropical Cyclone Cimatology. Obtenido de Tropical Cyclone Cimatology. available at: https://www.nhc.noaa.gov/climo/

NOAA. (2020b). NCEI OSTM/Jason-2 and Jason-3 Satellite Products Archive. Obtenido de NCEI OSTM/Jason-2 and Jason-3 Satellite Products Archive. Available at: https://www.nodc.noaa.gov/SatelliteData/jason/

Nystuen J, Andrade C (1993) Tracking mesoscale ocean features in the Caribbean Sea using Geosat Altimetry. J Geophys Res 98:8389–8394

Ortiz J, Plazas J, Lizano O (2015) Evaluation of Extreme Waves Associated with Cyclonic Activity of San Andrés in the Caribbean Sea since 1900. J Coast Res 31:557–568

Palanisamy H, Becker M, Meyssignac B, Henry O, Cazenave A (2012) Regional sea level change and variability in the Caribbean Sea since 1950. Journal of Geodetic Science 2:125–133

Penduff T, Melanie J, Brodeau L, Smith G, Barnier B, Molines J, Treguier A, Madec G (2010) Impact of global ocean model resolution on sea-level variability with emphasis on interannual time scales. Ocean Sci 6:269–284

Peterson T, Taylor M, Demeritte R, Duncombe D, Burton S, Thompson F, Porter A, Mercedes M, Villegas E, Fils R, Tank A, Martis A, Warner R, Joyette A, Mills W, Alexander L, Gleason B (2002) Recent changes in climate extremes in the Caribbean region. J Geophys Res 107:30–42

Richardson P (2005) Caribbean Current and eddies as observed by surface drifters. Deep-Sea Res II Top Stud Oceanogr 69:429–463

Rodriguez-Vera G, Romero-Centeno R, Castro C, Castro V (2019) Coupled Interannual Variability of Wind and Sea Surface Temperature in the Caribbean Sea and the Gulf of Mexico. J Clim 32:4263–4280

Ruiz M, Beier E (2012) Sea surface temperature variability in the Colombian Basin. Caribbean Sea Deep Sea Research 64:43–53

Saravanan R, Lakshmanan R, Jasmine S, Joshi K (2017) Coral bleaching: causes, consequences and mitigation. Marine Fisheries Information Service 231:1–9

Saunders M, Lea A (2008) Large contribution of sea surface warming to recent increase in Atlantic hurricane activity. Nature. 451:557–560

Schleussner C, Lissner T, Fischer E, Wohland J, Perrette M, Golly A, Rogelj J, Childers K, Schewe J, Friele K, Mengel M, Hare W, Schaeffer M (2016) Differential climate impacts for policy-relevants limits to global warming: the case of 1.5 °C and 2 °C. Earth System Dynamics 7:327–351

Sen-Gupta A, Jourdain N, Brown J, Monselesan D (2013) Climate Drift in the CMIP5 Models. J Clim 26:8597–8615

Serazin G, Penduff T, Grégorio S, Barnier B, Molines J, Terray L (2015) Intrinsic Variability of Sea Level from Global Ocean Simulations: Spatiotemporal Scales. J Clim 28:4279–4292

Sheng J, Tang L (2003) A Numerical Study of Circulation in the Western Caribbean Sea. J Phys Oceanogr 33:2049–2069

Stephenson T, Vincent L, Allen T, Van Meerbeeck C, McLean N, Peterson T, Taylor M, Aaron-Morrison A, Auguste T, Bernard D, Boekhoudt J, Blenman R, Braithwaite G, Brown G, Butler M, Cumberbatch C, Etienne-Leblanc S, Lake D, Martin D, Adrian T (2014) Changes in extreme temperature and precipitation in the Caribbean region, 1961-2010. Int J Climatol 34:2957–2971

Taylor M, Clarke L, Centella A, Bezanilla A, Stephenson T, Jones J, Campbell J, Vichot A, Charlery J (2018) Future Caribbean Climates in a World of Rising Temperatures: The 1.5 vs 2.0 Dilemma. J Clim 31:2907–2926

Tokyo Climate Center. (2020). Global Sea Surface Temperature Data Sets. Obtenido de Global Sea Surface Temperature Data Sets. Available at: http://ds.data.jma.go.jp/tcc/tcc/products/elnino/cobesst/cobe-sst.html

Torres R, Tsimplis M (2012) Seasonal sea level cycle in the Caribbean Sea. J Geophys Res Oceans 117:3304–3320

Torres R, Tsimplis M (2013) Sea-level variability in the Caribbean Sea over the last century. J Geophys Res Oceans 118:2934–2947

Torres R, Tsimplis M (2014) Sea level extremes in the Caribbean Sea. J Geophys Res Oceans 119:4714–4731

Torres R, Sánchez D, Moreno M (2017) Variación estacional del nivel del mar en el Archipiélago de San Andrés, Providencia y Santa Catalna. Mar Caribe Revista de Biología Marina y Oceanografía 52:343–352

UNCLOS, (1994). Agreement relating to the implementation of Part XI of the convention. Available at: https://www.un.org/Depts/los/convention_agreements/texts/unclos/closindxAgree.htm

United Nations. (2020). Sustainable Development Goals. Obtenido de Sustainable Development Goals. Available at: https://www.un.org/sustainabledevelopment/climate-action/

van Westen R, Dijkstra H, van der Boog C, Katsman C, James R, Bouma T, kleptsova O, Klees R, Riva R, Slobbe D, Zijlema M, Pietrzak J. (2020) Ocean model resolution dependence of Caribbean sea-level projections. Sci Rep 10:14599

Vuuren D., Edmonds J., Kainuma M., Riahi K., Thomson A., Hibbard K., Hurtt G., Kram T., Krey V., Lamarque, J., Masui T., Meinshausen M., Nakicenovic N., Smith S., Rose S. 2011. The representative concentration pathways: an overview. Climatic Change. This issue. Climatic Change, 109**:** 5-31.

Wang C, Lee S (2007) Atlantic warm pool, Caribbean Low-Level Jet, and their potential impact on Atlantic hurricanes. Geophys Res Lett 34:10–25

Watanabe M, Suzuki T, O'ishi R, Komuro Y, Watanabe S, Emori S, Takemura T, Chikira M, Ogura T, Sekiguchi M, Takata K, Yamazaki D, Yokohata T, Nozawa T, Hasumi H, Tatebe H, Kimoto M (2010) Improved Climate Simulation by MIROC5: Mean States, Variability, and Climate Sensitivity. J Clim 23:6312–6335

Yin J (2012) Century to multi-century sea level rise projections from CMIP5 models. Geophys Res Lett 39:17–35

Yoo J-M, Carton J (1990) Annual and Interannual Variation of the Freshwater Budget in the Tropical Atlantic Ocean and the Caribbean Sea. J Phys Oceanogr 20:831–845